



National Library  
of Canada

Bibliothèque nationale  
du Canada

Canadian Theses Service    Service des thèses canadiennes

Ottawa, Canada  
K1A 0N4

## NOTICE

The quality of this microform is heavily dependent upon the quality of the original thesis submitted for microfilming. Every effort has been made to ensure the highest quality of reproduction possible.

If pages are missing, contact the university which granted the degree.

Some pages may have indistinct print especially if the original pages were typed with a poor typewriter ribbon or if the university sent us an inferior photocopy.

Reproduction in full or in part of this microform is governed by the Canadian Copyright Act, R.S.C. 1970, c. C-30, and subsequent amendments.

## AVIS

La qualité de cette microforme dépend grandement de la qualité de la thèse soumise au microfilmage. Nous avons tout fait pour assurer une qualité supérieure de reproduction.

S'il manque des pages, veuillez communiquer avec l'université qui a conféré le grade.

La qualité d'impression de certaines pages peut laisser à désirer, surtout si les pages originales ont été dactylographiées à l'aide d'un ruban usé ou si l'université nous a fait parvenir une photocopie de qualité inférieure.

La reproduction, même partielle, de cette microforme est soumise à la Loi canadienne sur le droit d'auteur, SRC 1970, c. C-30, et ses amendements subséquents.

UNIVERSITY OF ALBERTA  
MODELS TO PREDICT LIGHTNING OCCURRENCE  
AND FREQUENCY OVER ALBERTA

BY

KERRY ROBERT ANDERSON



A thesis submitted to the Faculty of Graduate Studies and Research in partial fulfillment of the requirements for the degree of MASTER OF SCIENCE

IN

METEOROLOGY

DEPARTMENT OF GEOGRAPHY

EDMONTON, ALBERTA

FALL 1991



National Library  
of Canada

Bibliothèque nationale  
du Canada

Canadian Theses Service    Service des thèses canadiennes

Ottawa, Canada  
K1A 0N4

The author has granted an irrevocable non-exclusive licence allowing the National Library of Canada to reproduce, loan, distribute or sell copies of his/her thesis by any means and in any form or format, making this thesis available to interested persons.

The author retains ownership of the copyright in his/her thesis. Neither the thesis nor substantial extracts from it may be printed or otherwise reproduced without his/her permission.

L'auteur a accordé une licence irrévocable et non exclusive permettant à la Bibliothèque nationale du Canada de reproduire, prêter, distribuer ou vendre des copies de sa thèse de quelque manière et sous quelque forme que ce soit pour mettre des exemplaires de cette thèse à la disposition des personnes intéressées.

L'auteur conserve la propriété du droit d'auteur qui protège sa thèse. Ni la thèse ni des extraits substantiels de celle-ci ne doivent être imprimés ou autrement reproduits sans son autorisation.

ISBN 0-315-70086-6

UNIVERSITY OF ALBERTA

RELEASE FORM

NAME OF AUTHOR: Kerry Anderson

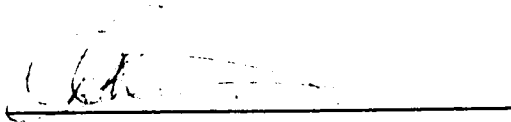
TITLE OF THESIS: Models to Predict Lightning Occurrence and Frequency  
over Alberta

DEGREE: Master of Science in Geography  
(specialization in Meteorology)

YEAR THIS DEGREE IS GRANTED: 1991

Permission is hereby granted to the University of Alberta Library to reproduce single copies of this thesis and to lend or sell such copies for private, scholarly or scientific research purposes only.

The author reserves all other publication and other rights in association with the copyright in the thesis, and except as hereinbefore provided neither the thesis nor any substantial portion thereof may be printed or otherwise reproduced in any material form whatever without the author's prior written permission.




Kerry Robert Anderson  
11249 93 Street  
Edmonton, Alberta  
Canada T5G 1B9

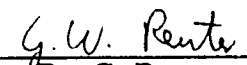
October 10, 1991

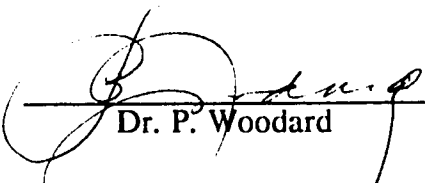
UNIVERSITY OF ALBERTA

FACULTY OF GRADUATE STUDIES AND RESEARCH

The undersigned certify that they have read, and recommended to the Faculty of Graduate Studies and Research for acceptance, a thesis entitled MODELS TO PREDICT LIGHTNING OCCURRENCE AND FREQUENCY OVER ALBERTA submitted by Kerry Robert Anderson in partial fulfillment of the requirements for the degree of MASTER OF SCIENCE in METEOROLOGY.

  
\_\_\_\_\_  
Dr. R.B. Charlton  
Supervisor

  
\_\_\_\_\_  
Dr. G. Reuter

  
\_\_\_\_\_  
Dr. P. Woodard

October 10, 1991

## TABLE OF CONTENTS

CHAPTER 1 INTRODUCTION .....	1
1.1 Forward .....	1
1.2 Overview of Lightning .....	3
a. Thundercloud Structure .....	3
b. Theories of Charge Generation in Thunderclouds .....	6
c. The Lightning Flash .....	8
1.3 Lightning Detection .....	10
CHAPTER 2 METHODOLOGY .....	13
2.1 Introduction .....	13
2.2 The General Thunderstorm Model .....	14
a. Convective Processes .....	14
b. Dynamic Processes .....	19
c. Charge Generation Processes .....	20
2.3 Data Sources .....	22
2.4 The Statistical Study .....	24
a. <i>t</i> Tests .....	28
b. Logistic Regression .....	30
c. Linear Regression .....	33
d. Multiple Linear Regression .....	33
2.5 The Map Study .....	34
a. Composite Map Study .....	35
b. Case Study .....	37
CHAPTER 3 STATISTICAL STUDY OF LIGHTNING OCCURRENCE AND FREQUENCY .....	39
3.1 Introduction .....	39
3.2 Occurrence and Non-occurrence of Lightning .....	39
a. <i>t</i> Test .....	39
b. Logistic Regression .....	45
3.4 Frequency of Lightning Flashes .....	50
a. Linear Regression .....	51
b. Multiple Linear Regression .....	53
CHAPTER 4 MAP ANALYSIS OF AREAS OF INTENSE LIGHTNING ..	60
4.1 Introduction .....	60
4.2 Composite Map Study .....	60
4.3 A Case Study .....	63
CHAPTER 5 CONCLUSIONS .....	75
5.1 Conclusions .....	75
5.2 Further Research .....	77

BIBLIOGRAPHY .....	79
APPENDIX A DERIVATION OF THE LIFTED SURFACE TEMPERATURE .....	83
APPENDIX B DERIVATION OF THE LIFTED 850 MB TEMPERATURE .....	85
APPENDIX C DERIVATION OF THE ISOBARIC WET-BULB TEMPERATURE .....	87
APPENDIX D LIGHTNING FREQUENCY FOR STONY PLAIN BETWEEN 12:00 UTC AND 00:00 UTC, 1986 .....	89
APPENDIX E LIGHTNING FREQUENCY FOR STONY PLAIN BETWEEN 12:00 UTC AND 00:00 UTC, 1987 .....	90
APPENDIX F LIGHTNING FREQUENCY FOR STONY PLAIN BETWEEN 12:00 UTC AND 00:00 UTC, 1988 .....	91

## LIST OF TABLES

Table 2.1. Data sources used in study. . . . .	22
Table 2.2. Parameter descriptions and statistics. . . . .	26
Table 2.3. Parameters used in predictive models. . . . .	27
Table 2.4. Assigned values and descriptions for parameter contribution to lightning. . . . .	37
Table 3.1. <i>t</i> test results for days with lightning versus days without lightning. . . . .	41
Table 3.2. Model 1: logistic regression of days with lightning versus days with no lightning. . . . .	46
Table 3.3. Model 2: logistic regression of days with lightning versus days with no lightning. . . . .	47
Table 3.4. Skill scores for the logistic regression models. . . . .	49
Table 3.5. Skill scores for the verification of the logistic regression models. . .	50
Table 3.6. Correlation coefficients for linear regressions of parameters against the number of lightning flashes. . . . .	52
Table 3.7. Model 1: stepwise linear regression to predict the total number of flashes using data for days with lightning and days with no lightning. . .	54
Table 3.8. Model 2: stepwise linear regression to predict the total number of lightning flashes using only data for days with lightning. . . . .	55
Table 3.9. Model 3: stepwise linear regression to predict the logarithm of the total number of lightning flashes using only data for days with lightning. . . . .	56
Table 3.10. Paired <i>t</i> test values of verification of multiple linear regression models. . . . .	58
Table 4.1. Parameter significance . . . . .	61
Table 4.2. Ranked listing of significant features with more than 10% occurrence. . . . .	62
Table A.1. Temperatures at selected pressure levels following pseudoadiabatic expansion. . . . .	83
Table A.2. Nonlinear regression results . . . . .	84
Table B.1. Temperatures at selected pressure levels following pseudoadiabatic expansion. . . . .	85
Table B.2. Polynomial regression results. . . . .	86



## LIST OF FIGURES

Figure 1.1. Typical charge distribution within a thundercloud. . . . .	4
Figure 1.2. The non-inductive ice-ice process. . . . .	7
Figure 1.3. The Alberta Forest Service's LLP direction finder network. . . . .	12
Figure 1.4. Lightning detection map for June 22, 1988. . . . .	12
Figure 2.1. The general thunderstorm model. . . . .	14
Figure 2.2. The <i>t</i> test measures the significance of the difference of the means of two populations. . . . .	29
Figure 2.3. The logistic regression curve. . . . .	31
Figure 2.4. Alberta Weather Centre's severe weather parameters and symbols. . . . .	35
Figure 4.1. Lightning detection map for June 21, 1988. . . . .	64
Figure 4.2. Lightning detection map for June 22, 1988. . . . .	64
Figure 4.3. Lightning detection map for June 23, 1988. . . . .	64
Figure 4.4. Lightning detection map for June 24, 1988. . . . .	64
Figure 4.5. Composite map for 00:00 UTC June 23, 1988. . . . .	67
Figure 4.6. Composite map for 12:00 UTC June 23, 1988. . . . .	67
Figure 4.7. Composite map for 00:00 UTC June 24, 1988. . . . .	67
Figure 4.8. Composite map for 12:00 UTC June 24, 1988. . . . .	67
Figure 4.9. Lightning centre tracks for June 22, 1988. . . . .	68
Figure 4.10. Lightning centre tracks for June 23, 1988. . . . .	68
Figure 4.11. Negative lightning occurrence prediction map for 12:00 UTC June 22, 1988. . . . .	70
Figure 4.12. Negative lightning occurrence prediction map for 00:00 UTC June 23, 1988. . . . .	70
Figure 4.13. Negative lightning occurrence prediction map for 12:00 UTC June 23, 1988. . . . .	70
Figure 4.14. Negative lightning occurrence prediction map for 00:00 UTC June 24, 1988. . . . .	70
Figure 4.15. Negative lightning occurrence prediction map for 12:00 UTC June 24, 1988. . . . .	70
Figure 4.16. Negative lightning occurrence prediction map for 00:00 UTC June 25, 1988. . . . .	70

## ABSTRACT

This thesis sets out to build a scheme to forecast lightning over Alberta. This was accomplished through the development of lightning occurrence and frequency prediction models. These models were built using statistical modeling and map analysis.

A number of statistical tests were conducted on lightning data using upper air data from Stony Plain, Alberta as predictors. Lightning data from two summers were compiled from the Alberta Forest Service's LLP lightning detection system. Lightning flashes located within an area around the Stony Plain upper air station were totalled to give daily positive and negative lightning flash frequencies. Statistical tests were conducted using 00:00 UTC (6:00 LDT) and 12:00 UTC (18:00 LDT) upper air parameters as predictors. The following tests were included:  $t$  tests to determine the significance of each predictor at discriminating days with lightning from days with no lightning; stepwise logistic regressions to predict the probability of lightning occurrence; linear regressions to determine the significance of each predictor at explaining lightning frequency; and stepwise linear regressions to predict lightning frequency and the logarithm of lightning frequency.

Results from the aforementioned tests showed that convective indices are the best predictors of both lightning occurrence and frequency. Logistic regression models correctly predicted lightning occurrence above an 80% accuracy. Linear

regression models explain between 20% and 40% of the variance of lightning frequency. These results confirm the convective nature of lightning; however, the poor correlations imply that something more than upper air parameters are needed to forecast lightning frequency reliably.

A map study was conducted, which compared severe weather composite maps provided by the Alberta Weather Centre to lightning detection maps produced by the AFS LLP lightning detection system. This study reinforces the conclusions from the statistical study in that convection is the best predictor of lightning of all variables studied. Spatial predictions of lightning occurrence were produced using the logistic regression equations and interpolations of observations from the upper air stations in and around Alberta. A case study shows that this approach is valid and, if considered along with the composite map results, can be used to produce acceptable short range forecasts.

# CHAPTER 1

## INTRODUCTION

### 1.1 Forward

Lightning is one of the most spectacular meteorological phenomena and the most common severe weather event to affect mankind directly. But despite decades of research and advances in instrumentation, the exact origin of lightning and the mechanisms behind the charge buildup in a thundercloud are still not understood (Dye 1990; Williams 1988; Krider and Alejandro 1983).

The problem confronting lightning research is the range of scales the phenomenon encompasses. Processes at the molecular level must be combined with those at the scale of the troposphere and greater. Though progress has been made to understand specific processes, putting them together into the "big picture" has eluded the research community.

Without a firmly established understanding of the principles behind cloud electrification, weather forecasters have only a superficial knowledge of lightning. They know that lightning is generally associated with convective activity and it has been assumed that methods of predicting other convective phenomena, such as rain showers and hail, should work well for predicting lightning. As a result, only a few

predictive techniques have been devised to forecast lightning specifically (Sly 1966; Fuquay 1980; Andersson *et al.* 1989; Reap 1990).

During the last decade, lightning detection systems have given meteorologists a new source of data. These systems provide real time data of lightning occurrence and its location. But, like a Pandora's box, lightning detection systems have created more questions than answers as observers begin to look at lightning with a new degree of resolution.

Is the intensity of lightning activity directly correlated with the intensity of convection? Observations do not seem to support this. The experience in Alberta is that although indicators of convective instability point to thunderstorm activity, there is no way of determining whether a storm will yield 1,000 or 10,000 lightning flashes (Nimchuck 1985).

The forest industry has a definite need for lightning forecasts. Lightning is a major cause of forest fires, starting 34%<sup>1</sup> (3,101) of the near 10,000 fire occurrences annually in Canada. Lightning-caused fires account for 87% (1,840,822 ha) of total area burned nationwide. The discrepancy in the percentages is due to the general inaccessibility of lightning-caused fires. As a result, a large number of them escape

---

<sup>1</sup>Figures based on a 10-year annual average for 1973 to 1982 for the 10 provinces and two territories (Ramsey and Higgins 1986).

the initial containment attempts. Consequently, forest protection agencies are a main user of lightning detection systems.

This research sets out to build models to predict lightning occurrence and frequency over Alberta. Statistical regression techniques are used to predict the probability of lightning occurrence and the expected number of lightning flashes from upper air soundings. The regression equations are then applied to interpolated upper air fields to producing spatial predictions of lightning activity. Finally, the prediction fields are modified by severe weather analysis schemes to arrive at the final forecast.

## **1.2 Overview of Lightning**

This section presents a brief overview of the basic theories and observations of thundercloud electrification and the lightning discharge. For a more comprehensive background, the reader should consult textbooks by Chalmer (1967), Uman (1987), and Golde (1977), and papers by Latham (1981), Uman and Krider (1982, 1989), and Williams (1985).

### **a. Thundercloud Structure**

Lightning is generally associated with convective weather activity. Thunder, and therefore lightning, is used by the professional weather observer to classify the severity of convective activity. Cumulonimbus clouds are the largest form of

convective cloud and typically produce lightning. Cumulonimbus clouds with lightning activity are generally referred to as thunderclouds.

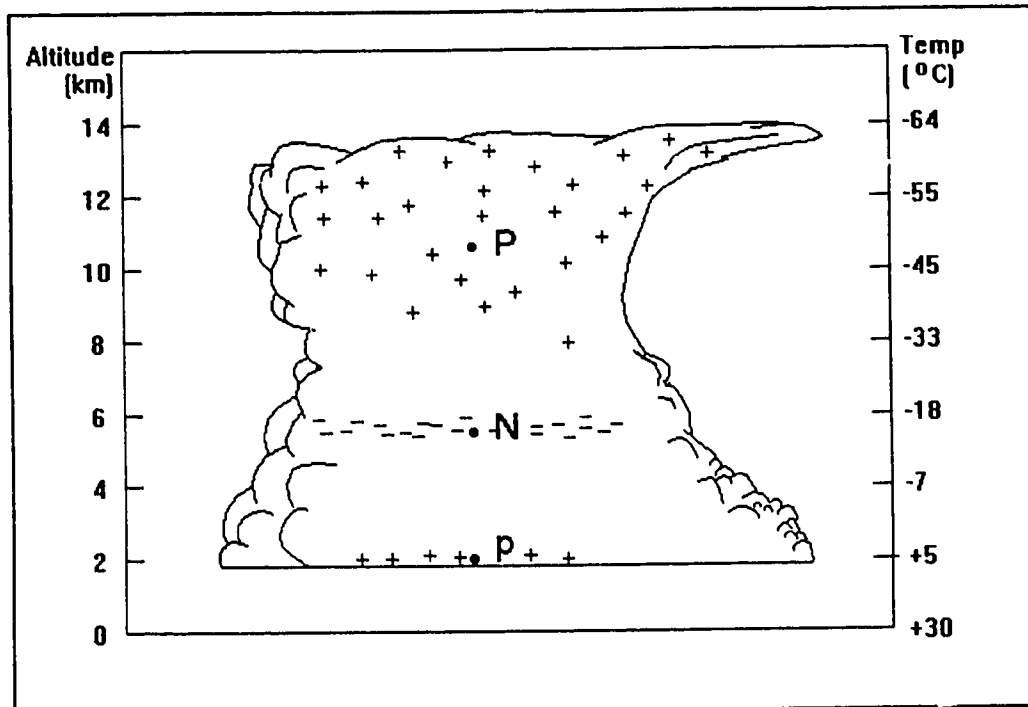


Figure 1.1. Typical charge distribution within a thundercloud.

The classic thundercloud model, shown in Figure 1.1, consists of a positive electric dipole with a positively charged region above a negatively charged region (Wilson 1920). An additional weak region of positive charge exists at the cloud base (Simpson and Robinson 1941; Simpson and Scrase 1937). The three centres of accumulated charge are labelled P, N, and p, respectively. The P and the N regions have approximately equal and opposite charge, creating the positive dipole. Malan (1963) documented charges and altitudes above ground level for the p, N, and P

regions of a typical South African thundercloud (1.8 km ASL) as +10 C (coulombs) at 2 km, -40 C at 5 km, and +40 C at 10 km. These are representative of values that can vary considerably with geography and from cloud to cloud.

Research by Krehbiel *et al.* (1983; 1984) and MacGorman and Taylor (1981) on the charge structure of lightning discharges has further identified the nature of the negative charge region. General findings indicate that the negative charge region in a thundercloud is located in a subfreezing region of small vertical dimension (less than a kilometre) somewhere between -10 and -25 °C (Krehbiel *et al.* 1983). Krehbiel noted further that the altitude of the negative charge centre remained constant throughout the storm growth and was not affected by the strength of the vertical wind.

The positive charge region higher up in the cloud follows a different set of characteristics. Krehbiel's study found that the positive charge region did rise steadily with time at a speed of approximately 8 m/s. MacGorman *et al.* (1984) noted that positive flashes occurred most frequently in the mature to late stages of growth in individual convective cells. He also noted that these flashes tended to occur in the forward swept anvil of the cloud and the stratiform layer following the cell. These observations have been supported by several other studies (Holle *et al.* 1985; Stolzenburg 1990; Lopez *et al.* 1990; Holle *et al.* 1990; Hunter *et al.* 1990). These studies suggest that the positively charged particles are carried by the



convective currents in the cloud and that positive flashes are more likely to occur when the charge region is horizontally displaced from the negatively charged region.

#### **b. Theories of Charge Generation in Thunderclouds**

Several theories have been developed to explain the charge generation in a thundercloud. They fall into two general categories: convective and gravitational.

Convective theories propose that free ions in the atmosphere are captured by cloud droplets and are then moved by the convective currents in the cloud to produce the charged regions. Although convective theories have merit, they fail to describe observed characteristics of the thundercloud, such as the stratified characteristic of the negative charge centre.

Among the scientific community, gravitational theories are preferred. They assume that negatively charged particles are heavier and are separated from lighter, positively charged particles by gravitational settling. For gravitational theories to work, there must be some charge exchange process between particles of different sizes. Charge can be exchanged between particles by inductive and non-inductive processes. Dye (1990) and Illingworth (1983) provide comprehensive reviews of these processes. The most promising is the non-inductive exchange between ice crystals and hailstones, referred to as the ice-ice process (Reynolds *et al.* 1957).

The effectiveness of the ice-ice process lies in the thermo-electric properties of ice (see Figure 1.2). The mobility of the  $(\text{OH}_3)^+$  defect in ice is greater than the  $(\text{OH})^-$  defect and the number of defects increase with temperature. When warm and cold ice particles come in contact, the positive

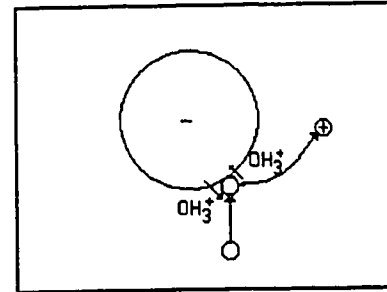


**Figure 1.2.** The non-inductive ice-ice process.

defect flows faster from the warmer to the colder particle than the converse giving the colder particle a net positive charge. In the typical scenario, therefore, a warm hailstone or snow pellet will acquire a net negative charge as it falls through a region of cold ice crystals.

Theories of thundercloud charge generation are still speculative. The favourability of one process over another has fluctuated over time because of the inadequate number of laboratory experiments and scarcity of useful field observations (Latham 1981; Williams 1985). *One clear conclusion is that there is no unique mechanism to generate the required charge under all conditions.* For example, the ice-ice process does not explain warm cloud lightning, albeit a not too frequent event. As research continues, the most likely explanation will lie in a combination of both general theories.

### **c. The Lightning Flash**

Lightning can occur in four ways. It can travel between points within a cloud, from a cloud to clear air, from a cloud to an adjacent cloud, and from a cloud to ground. These flashes are referred to as intracloud, cloud-to-air, cloud-to-cloud, and cloud-to-ground, respectively.

Cloud-to-ground (CG) flashes make up about 40% of lightning flashes (Uman and Krider 1989). The cloud-to-ground lightning flash can lower positive (+CG) or negative (-CG) charge, depending on the source of the flash. This can be determined by the polarity of the stroke's current.

The negative cloud-to-ground flash lowers negative charge from the negative charge centre to the ground. The flash begins with the stepped leader, a small packet of negative charge that descends from the cloud along the path of least resistance. Its motion is slow and sporadic, taking steps in the order of tens of metres in length and microseconds in duration. As the leader approaches the ground, streamers of positive charge reach out to the approaching leader. On contact, a powerful return stroke is triggered. This stroke moves upward, stripping negative charge from the ionized trail of the stepped leader. After the return stroke, the lightning flash may end or, if sufficient charge is collected in the cloud, a dart leader may descend to the ground triggering another return stroke. A typical lightning flash in northern latitudes consists of 3 or 4 return strokes (Uman 1987).

The positive cloud-to-ground flash is less common than the negative. Coming from higher altitudes in the cloud, positive flashes make up about 10% of all lightning flashes (Uman and Krider 1989). They are usually composed of a single stroke, and carry about 10 times more current. From the forestry perspective, positive flashes are of more concern as the higher currents are more likely to ignite fires.

Several studies have concentrated on the characteristics of the positive flash but results are inconclusive because of the number of observations. The percentage of positive flashes appears to increase with latitude (Takeuto *et al.* 1983) and with the height of local terrain (Uman and Krider 1989). Also, positive flashes are more common in winter storms (Takeuto *et al.* 1983; Williams 1988). The apparent cause for this is that the lower freezing level places the positive charge centre closer to the ground thus increasing the likelihood of a flash.

Positive flashes appear to be more common in stratiform clouds while negative flashes tend to occur in areas of strong convection (Holle *et al.* 1988). Also, thunderstorms that consist predominantly of negative flashes in their early stages, often end with positive discharges as the storm matures and the anvil spreads out (MacGorman *et al.* 1984).

A popular theory is that horizontal wind shears force a tilting of the dipole axis providing a route for the positive flash (Takeuto *et al.* 1983; Rust and MacGorman 1985) but this has yet to be shown conclusively.

### **1.3 Lightning Detection**

The Alberta Forest Service (AFS) uses the wide band magnetic gate design lightning detector (Krider *et al.* 1976, 1980; Hermann *et al.* 1976) manufactured by Lightning Location and Protection Inc. (LLP) of Tucson, Az. The LLP lightning detection system determines the time and location of a lightning flash by triangulating information from direction finders linked in a detection network. These data are stored on magnetic tape. Maps can be processed to show the location and polarity of lightning flashes that occur over time.

The LLP lightning detection system consists of three components: the direction finder, the position analyzer, and the remote display processor.

The direction finder (DF) senses the electromagnetic field radiated by a lightning flash using two erect, orthogonal wire loop antennas and a horizontal flat plate antenna. The antennas' bandwidths are from 1 kHz to 1 MHz. The radiated field of a lightning flash induces a current in the loops. The voltage signal measured in the loops is related to the flash's generated magnetic field strength by the cosine of the angle between the loop antenna and the direction to the flash. By comparing

the voltage signals from the two loops, a direction to the flash can be determined. The flat plate antenna measuring the electric field is used to resolve the 180 degree ambiguity associated with the two polarities of lightning flashes.

The direction finder can discriminate a cloud-to-ground flash from other forms of lightning or noise by electromagnetic signature. When the stepped leader reaches the ground, the return stroke is triggered producing a sharp voltage rise. This rise is used to distinguish a cloud-to-ground flash from other electromagnetic noise.

The direction finder sends the data of each registered lightning flash to a centralized position analyzer (PA). The position analyzer triangulates data from direction finders to locate the position of a lightning flash. If the flash is in line with or directly between two direction finders (called the baseline), the position analyzer considers the ratio of the signal strengths as well.

From the position analyzer, users can view a map of the lightning data on a remote display processor (RDP). The display can focus on desired time and location windows covered by the detection network and can show up to 30,000 flashes at a time.

The quality of data from the LLP lightning detection system has received much attention. The manufacturers claim 80% detection within a 400 km radius of

a detector and a 2 degree accuracy in the direction, although a recent study (Mach *et al.* 1986) found accuracy figures of only 70% detection within a 350 km range.

The Alberta Forest Service's LLP direction finder network, shown in Figure 1.3, consists of 16 direction finders situated in and around the province. The position analyzer is located at the AFS's provincial headquarters in Edmonton. Remote display processors (not shown in the figure) are located in the headquarters office, each of the AFS's 10 forest ranger stations, and in the offices of other agencies that are interested in the data, such as the Alberta Weather Centre. A sample lightning detection map is shown in Figure 1.4.

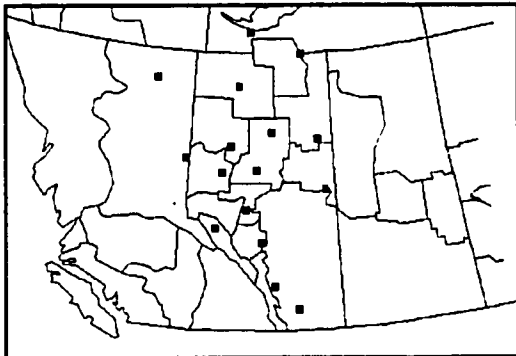


**Figure 1.3.** The Alberta Forest Service's LLP direction finder network.

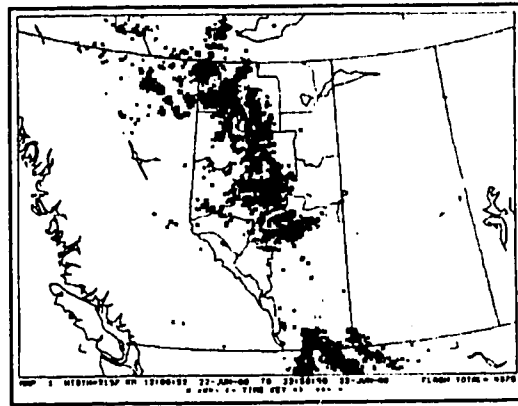


**Figure 1.4.** Lightning detection map for June 22, 1988.

## CHAPTER 2

### METHODOLOGY

#### 2.1 Introduction

The goal of this research is to produce models to predict lightning occurrence and frequency over Alberta. This will be accomplished through statistical modeling and map analysis.

Statistical tests, such as the  $t$  test, will indicate the relative importance of individual parameters to forecasting lightning. From this information, regression techniques will be used to build models to predict the probability of lightning occurrence and the expected number of lightning flashes from upper air soundings. The models will then be applied to interpolated upper air fields, producing a spatial prediction of lightning activity.

Map analysis will provide a means to evaluate features that do not lend themselves to statistical study. Features such as thermal ridges and axes of strong winds are represented on severe weather composite maps. They will be used to modify the spatial analysis produced by the regression equations to arrive at the final forecast. Finally, a case study will be used to evaluate the performance of the spatial prediction models.



## 2.2 The General Thunderstorm Model

The theories and observations discussed in Chapter 1 must be incorporated with convective weather theories to produce a general thundercloud model that can be used to predict lightning. Figure 2.1 illustrates the essential processes involved in this model. They can be broken down into three general categories: convective, dynamic, and charge generation processes.

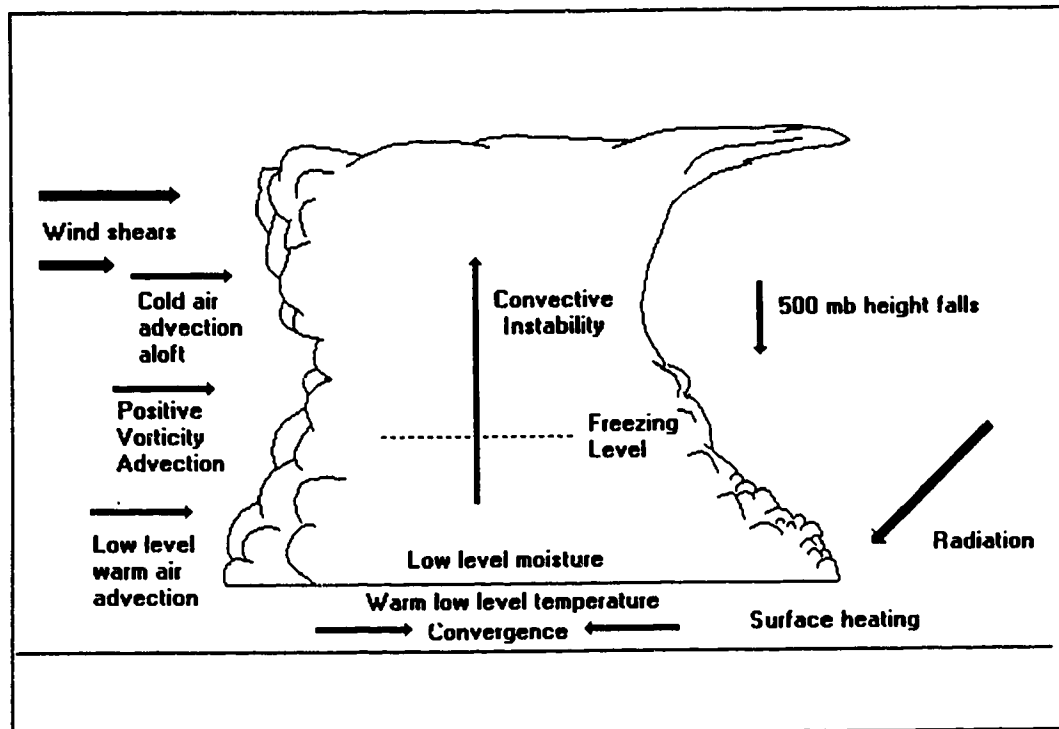


Figure 2.1. The general thunderstorm model.

### a. Convective Processes

Convective processes are the processes that promote atmospheric convection. These include convective instability, cold air advection aloft, low-level warm air advection, low-level moisture, surface heating, and radiation.

Seven convective indices have been chosen to represent convective instability. Convective indices are simple calculations of atmospheric instability that can be done by the forecaster. The convective indices used in this study are:

1. George's K Index:

$$K = (T_{850} - T_{500}) + (T_{d_{450}}) - (T_{700} \cdot T_{d_{700}}) \quad (2.1)$$

2. Simplified K Index:

$$K_2 = (T_{850} - T_{500}) + (T_{d_{450}}) \quad (2.2)$$

The simplified K index is the George's K index less the 700 mb moisture term. The simplified K index is not a recognized index -- the author has created it for comparative purposes in this study.

3. Vertical Totals Index:

$$VT = T_{850} - T_{500} \quad (2.3)$$

4. Cross Totals Index:

$$CT = T_{d_{450}} - T_{500} \quad (2.4)$$

5. Total Totals Index:

$$TT - VT + CT - T_{850} + T_{d_{850}} - 2T_{500} \quad (2.5)$$

6. Lifted Index:

$$LI - T_{500} - T'_{sfc} \quad (2.6)$$

where  $T'_{sfc}$ , or the lifted surface temperature, is the temperature of a parcel mixed in the bottom 50 mb, lifted adiabatically and, upon saturation, lifted pseudoadiabatically to 500 mb.

7. Showalter Index:

$$SI - T_{500} - T'_{850} \quad (2.7)$$

where  $T'_{850}$ , or the lifted 850 mb temperature, is the temperature of a parcel when lifted adiabatically and, upon saturation, lifted pseudoadiabatically, from 850 mb to 500 mb.

Equations used for the Lifted and Showalter Indices are given by equations (2.8) and (2.9). Terms in the square brackets are regression equations for the appropriate lifted temperatures as calculated by the author. Derivation of these regressions are outlined in Appendices A and B.

$$LI - T_{500} - [0.9938T_{w_{sfc}} \left(\frac{500}{P_{sfc}}\right)^{-0.7138} - 10.4\left(\frac{500}{P_{sfc}}\right)^{-1.991}] \quad (2.8)$$

$$SI - T_{500} - [0.0042(T_{w_{550}})^2 + 1.3738T_{w_{550}} - 29.1241] \quad (2.9)$$

Temperatures are in degrees Celsius. The surface pressure is the actual station pressure (not MSL) in millibars. Equations are accurate to within half a degree Celsius.

Both equations (2.8) and (2.9) require the wet-bulb temperature as part of their solution. The equation used to calculate the isobaric wet-bulb temperature,  $T_{iw}$ , is

$$T_{iw} = T + 10^{9.4041} \frac{l_v \varepsilon}{c_p p} \left(10^{-\frac{2354}{T_d}} - 10^{-\frac{2354}{T_{iw}}}\right)$$

where (2.10)

$$\varepsilon = 0.622$$

$$l_v = 2.5008 \times 10^6 \text{ J kg}^{-1} \text{ at } 0^\circ\text{C}$$

$$c_p = 1005 \text{ J kg}^{-1}\text{K}^{-1}$$

All temperatures are in Kelvin and pressure is in millibars. Because the wet-bulb temperature is on both sides of the equation, the answer must be converged upon. Starting with an approximate wet-bulb temperature of the mean between the

dry-bulb temperature and the dew-point temperature, four iterations usually yield a wet-bulb temperature accurate to within half a degree. Derivation of equation (2.10) is explained in Appendix C.

There are other convective indices that have not been included in the study for various reasons. CAPE (convective available potential energy) is an index that measures the energy released to buoyancy as a parcel is lifted in the atmosphere. This is calculated by integrating the temperature difference between the lifted parcel and the environment for the length of desired lift in a sounding. Because this index requires sounding measurements, it cannot easily be represented spatially, defeating the purpose of this research.

Another index not included is the SWEAT (severe weather) index. A product of regression analysis of tornadic events, this index is used regularly to predict severe weather. But, because lightning is not considered a severe weather phenomenon, the SWEAT index was not considered in the study.

Low-level moisture, warm low-level temperatures and cold temperatures aloft are components of convective indices. They contribute to convective instability and can be looked at individually for further information.

Other parameters associated with convection that are included in the thunderstorm model, modify the convective instability with time. Cold air advection aloft, low-level warm air advection, and surface heating each tend to increase the instability of the atmosphere.

Solar radiation affects the surface heating rate, which influences convective instability. The actual radiation received at the surface is hard to measure and data are not readily available for direct incorporation into the model. A simplified relationship will be used to estimate the radiation as shown by

$$Q = \sin\left(2\pi \frac{(\text{Julian day}) - 80}{365}\right) \quad (2.11)$$

This equation shows the normalized departure from the average top of the atmosphere radiation received. It would reach its peak value of 1 on June 21 and its lowest value of -1 on December 21. The average top of the atmosphere radiation received is a constant that would be incorporated indirectly by any regression analysis. The equation assumes a constant latitude, which is adequate for this study.

#### **b. Dynamic Processes**

Two dynamic processes that force lift in an airmass have been included. These may be the necessary impetus to initiate convection. The processes are low-level horizontal convergence and mid-tropospheric positive vorticity advection.

The horizontal convergence over an area can be determined from surface winds by solving the equation

$$\text{Convergence} = -\nabla \cdot \vec{v}_h = -\left(\frac{\partial u}{\partial x} + \frac{\partial v}{\partial y}\right) \quad (2.12)$$

where  $u$  and  $v$  are the  $x$  and  $y$  surface wind components. In the boundary layer, horizontal convergence forces lift, which can initiate convection by breaking through the nocturnal inversion layer.

Vorticity advection, normally assessed at the 500 mb level, is an important dynamic process that produces vertical motion in the atmosphere through baroclinic instability. Positive vorticity advection (PVA) can trigger convective instability by tapping potential instability in the airmass.

### **c. Charge Generation Processes**

As discussed in Chapter 1, there are certain processes that appear to be important in generating charge in thunderclouds and initiating lightning. They include the freezing level, wind shears, and 500 mb height falls.

Ice plays an important role in generating charge in the thundercloud. Presumably, the altitude of the freezing level could determine the characteristics of lightning activity in the cloud. This is best represented by the wet-bulb zero (WBZ)

height. The wet-bulb zero height has long been recognized as a parameter important in determining the likelihood of severe weather activity (Miller 1967). It is the altitude where the ambient wet-bulb temperature equals 0°C. Height is measured as above ground level. The height of the wet-bulb zero determines the likelihood of severe weather reaching the ground. It has been observed that for most severe weather events, such as hail and tornadoes, the wet-bulb zero is restricted to between 5,000 and 11,000 feet (Miller 1967). Above this range, severe weather is not likely to affect the surface; below this range, severe weather is not likely to occur.

Vertical wind shears have been recognized as a possible mechanism to explain storms with a high number of positive cloud to ground flashes. They are believed to cause a tilt in the thundercloud's dipole axis giving the positive lightning flashes a direct route to the ground away from the negative charge centre.

The 500 mb height fall is a simple measurement that has been used successfully by the Alberta Forest Service to predict lightning-caused fire occurrences (Nimchuck 1983; Janz and Nimchuck 1985). It is an indirect measurement of the movement of upper troughs and thus baroclinic instability. In the summer months, when a ridge lies over a forested area for several days, ground fuels tend to dry under the hot, clear sky. As the ridge breaks down, lightning associated with the approach of the trough can cause many ignitions in the dry fuels and the high winds can create an extreme fire hazard situation. Although forest fire ignitions are outside



the realm of this thesis, the 500 mb height changes may be a worthwhile feature to examine.

### 2.3 Data Sources

Table 2.1 summarizes the data sources used in this thesis. The periods used in the study were based on data availability and on the months of peak lightning occurrence (May through August).

**Table 2.1. Data sources used in study.**

Data	Source	Mode	Period
Lightning data	AFS	Tape	May-1-86 to Aug-31-86 May-1-87 to Aug-31-87 May-1-88 to Aug-31-88
Daily lightning maps	AFS	Maps	May-1-86 to Aug-31-86 May-1-87 to Aug-31-87 May-1-88 to Aug-31-88 May-1-89 to Aug-31-89
Severe weather desk composite maps	AIWC	Maps	Jun-3-86 to Aug-26-86 May-27-88 to Jul-14-88 Jun-1-89 to Aug-26-89
Upper air soundings	CCC	Tape	May-1-86 to Aug-31-86 May-1-87 to Aug-31-87 May-1-88 to Aug-31-88
Upper air maps	CMC	Maps	May-1-86 to Aug-31-86 May-1-87 to Aug-31-87 May-1-88 to Aug-31-88

The AFS's lightning detection system collects lightning data 24 hours a day, year-round, for Alberta and surrounding area. The system records the time, the

location (latitude-longitude), the signal strength (including polarity), and the number of return strokes for each lightning flash detected. Lightning data were collected for May through August of the years 1986, 1987, and 1988.

At 6:00 MDT, the AFS produces a daily lightning map summarizing the lightning in the past 24 hours. Copies of these maps were collected for May through August of the years 1986, 1987, 1988, and 1989.

During the summer months, forecasters on the severe weather desk at the Alberta Weather Centre (AIWC) produce composite maps that help forecast areas of severe weather. These maps show features at various altitudes that lead to convection or lift. Maps for most of the days from late May through mid-August were collected for the years 1986, 1988, and 1989.

The Atmospheric Environment Service (AES) collects radiosonde data from various stations throughout Canada. Forty-five minutes before 00:00 and 12:00 UTC (Universal Coordinated Time), AES releases weather balloons (also known as radiosondes) that measure temperature, pressure, humidity, horizontal wind speed, and wind direction at various altitudes. Each collection of measurements from one balloon release is called a sounding. Individual soundings are plotted on tephigrams to show the variation of winds, pressure, temperature, and dew-point temperature with altitude.

Upper air sounding data are also available from the Canadian Climate Centre (CCC). There is about a one-year time lag in data availability to allow for quality control. The Canadian Climate Centre's Edmonton office provided a magnetic tape of the individual soundings. Stony Plain sounding data for May through August of the years 1986, 1987, and 1988 were used in this study.

The Canadian Meteorological Centre (CMC) uses sounding data to plot upper air maps. Upper air maps are plotted for 850 mb, 700 mb, 500 mb, and 250 mb and supplied over the facsimile circuit. The upper air maps used in the study are for May through September, 1986 and 1987, collected from the Alberta Weather Centre and the University of Alberta's facsimile circuit.

#### **2.4 The Statistical Study**

The aim of the statistical study is to determine the characteristics of lightning and to build regression equations to predict lightning occurrence and frequency using parameters taken from upper air soundings as the predictors.

The predictands of the study will be lightning occurrence and lightning frequency. Lightning occurrence will be defined as the occurrence of one or more lightning flashes of a given polarity within one degree latitude and longitude of Stony Plain between 12:00 and 23:59 LDT. Lightning frequency will be defined as the number of lightning flashes of a given polarity that occur within one degree latitude

and longitude of Stony Plain between 12:00 and 23:59 LDT. Daily lightning frequencies are tabulated in Appendices E, F, and G for 1986, 1987, and 1988. Data for the years 1986 and 1987 will be used to build predictive models. The 1988 data will be used for verification.

The predictor variables used in the statistical study are upper air sounding parameters taken from, or derived from, an individual upper air sounding. Table 2.2 lists all parameters and abbreviations used. As well, average values and standard deviations of the parameters are included. These variables will be studied to find any interesting characteristics of lightning.

Not all terms listed in Table 2.3 are acceptable or probable indicators of instability or lift. Upper air predictors that best approximate these processes in the proposed thundercloud model were used to build the predictive models. These parameters are listed in Table 2.3.

Table 2.2. Parameter descriptions and statistics.

Parameter	Description	Units	1200 UTC			0000 UTC		
			mean	st.dev.	N	mean	st.dev.	N
PTOT	Positive flash total	flashes	9.074	30.850	244	9.086	30.848	244
NTOT	Negative flash total	flashes	134.655	445.398	244	134.630	445.406	244
PTOT2	Previous day's positive flash total	flashes	9.140	30.969	242	9.161	30.964	242
NTOT2	Previous day's negative flash total	flashes	135.735	447.083	242	135.743	447.080	242
WBZ	Wet-bulb zero height	m	1735.011	663.988	243	1825.039	570.591	242
SfcPr	Surface pressure	mb	924.478	5.719	243	923.710	5.696	242
MSLPr	MSL pressure*	mb	1014.086	6.542	243	1010.475	6.364	242
ZS	1000 mb height	m	108.003	53.799	243	81.098	54.313	242
Z8	850 mb height	m	1468.228	52.631	243	1470.031	52.719	242
Z7	700 mb height	m	3050.990	61.406	243	3057.829	60.910	241
Z5	500 mb height	m	5656.293	89.506	243	5669.809	88.432	241
TS	Surface temperature	°C	9.787	3.871	243	18.441	5.219	242
T8	850 mb temperature	°C	9.922	4.970	242	11.596	4.863	242
T7	700 mb temperature	°C	-1.016	4.330	243	-0.227	4.397	241
T5	500 mb temperature	°C	-17.120	4.236	243	-16.601	4.019	241
TdS	Surface dew-point temperature	°C	6.658	4.212	243	6.101	5.305	242
Td8	850 mb dew-point temperature	°C	1.620	5.133	243	2.260	5.049	242
Td7	700 mb dew-point temperature	°C	-6.767	5.986	243	-7.152	5.376	241
Td5	500 mb dew-point temperature	°C	-26.734	7.299	243	-26.507	6.620	241
DDS	Surface dew-point depression	°C	3.129	3.085	243	12.341	5.930	242
DD8	850 mb dew-point depression	°C	8.346	5.200	242	9.335	5.345	242
DD7	700 mb dew-point depression	°C	5.751	5.577	243	6.926	5.538	241
DD5	500 mb dew-point depression	°C	9.614	6.536	243	9.906	5.902	241
F8	850 mb wind speed	km/h	30.801	18.935	241	22.874	14.326	240
F7	700 mb wind speed	km/h	32.578	16.640	241	33.749	15.869	240
F5	500 mb wind speed	km/h	48.197	26.799	242	50.624	27.297	240
TH8	850 mb wind direction	°	242.738	95.623	241	222.057	97.310	240
TH7	700 mb wind direction	°	248.787	81.643	241	257.046	66.784	240
TH5	500 mb wind direction	°	247.693	70.389	242	250.903	67.139	240
dPR	24-hour surface press change	mb	0.089	5.277	242	0.072	5.393	240
dZS	24-hour 1000 mb height change	m	0.661	51.677	242	0.483	53.736	240
dZ8	24-hour 850 mb height change	m	1.074	45.722	242	0.862	46.978	240
dZ7	24-hour 700 mb height change	m	1.438	45.534	242	0.929	46.423	238
dZ5	24-hour 500 mb height change	m	2.165	58.775	242	1.807	60.868	238
dTS	24-hour surface temperature change	°C	0.072	3.017	242	0.088	4.733	240
dT8	24-hour 850 mb temperature change	°C	0.109	4.353	240	0.043	4.454	240
dT7	24-hour 700 mb temperature change	°C	0.055	3.531	242	0.056	3.630	238
dT5	24-hour 500 mb temperature change	°C	0.061	3.248	242	0.074	3.061	238
TWS	Surface wet-bulb temperature	°C	8.154	3.578	243	11.630	3.612	242
TW8	850 mb wet-bulb temperature	°C	5.819	3.762	242	6.876	3.603	242
WS87	850-700 mb wind shear	km/h	45.576	29.481	241	39.940	23.175	240
WS75	700-500 mb wind shear	km/h	55.947	34.788	241	58.258	37.292	240
T87adv	850-700 mb temperature advection	°C/h	-0.010	0.483	241	0.026	0.450	240
T75adv	700-500 mb temperature advection	°C/h	-0.020	0.488	241	0.013	0.499	240
TH	1000-500 mb thickness	m	5548.293	85.073	243	5588.949	87.539	241
dTH	24-hour thickness change	m	1.504	63.483	242	1.433	68.595	238
K	George's K index	°C	22.864	8.789	242	23.560	7.604	241
K2	Modified K index	°C	28.631	5.973	242	30.485	5.765	241
VT	Vertical Totals	°C	27.055	3.297	242	28.207	3.398	241
CT	Cross Totals	°C	18.740	4.392	243	18.879	4.156	241
TT	Total Totals	°C	45.765	5.743	242	47.087	5.381	241
SI	Showalter index	°C	3.769	3.350	242	2.779	3.170	241
LI	Lifted index	°C	5.793	3.788	243	0.860	3.624	241
Q	Radiation	-	0.811	0.182	244	0.813	0.178	244

\* surface pressure is the pressure measured at the station

\*\* MSL pressure is the station pressure extrapolated to the surface

**Table 2.3. Parameters used in predictive models.**

Category	Process	Parameter	Description
Convection	Convective Instability	K	George's K index
		K2	Simplified K index
		VT	Vertical totals
		CT	Cross totals
		TT	Total totals
		SI	Showalter index
		LI	Lifted index
	Low-level temperature	TS	Surface temperature
		T8	850 mb temperature
	Low-level moisture	TdS	Surface dew-point temperature
		Td8	850 mb dew-point temperature
	Surface heating	Q	Radiation
		dTS	24-hour surface temperature change
	Warm air advection at low levels	T87adv	850-700 mb temperature advection
		dT8	24-hour 850 mb temperature change
	Cold air advection aloft	T75adv	700-500 mb temperature advection
dT5		24-hour 500 mb temperature change	
Charge generation and lightning	Freezing level	WBZ	Wet-bulb zero height
	500 mb height falls	dZ5	24-hour 500 mb height change
Additional	Persistence	PTOT2	Previous day's positive flash total
		NTOT2	Previous day's negative flash total
	Other	ZS	1000 mb height
		Z8	850 mb height

Each study will be conducted in four parts. As predictands, positive and negative flashes will be studied separately to determine any independent

characteristics. For prediction equations, 00:00 UTC and 12:00 UTC soundings will be studied separately to decide if morning (12:00 UTC) soundings are useful in determining the day's lightning, or if afternoon values (00:00 UTC), real or predicted, are needed.

The statistical study consists of four tests. These include the  $t$  test, logistic regression, linear regression, and multiple linear regression. All these tests are clearly described in most intermediate statistical texts such as Neter *et al.* (1985). The statistical analyses will be run using the 1988 version of BMDP -- a statistical software package for mainframe computers, produced by the University of California, Los Angeles.

#### **a. $t$ Tests**

The  $t$  test is a statistical test used to determine if, under the null hypothesis ( $H_0$ ), there are no differences between the means of two samples. In other words, the samples are taken from the same population, assuming a normal distribution. The converse of this, the alternate hypothesis ( $H_a$ ), assumes that the means are different and that the samples are from two distinct populations. Figure 2.2 illustrates the principle of the  $t$  test. The means and the variances of the two populations are compared to derive a  $t$  value, measuring the significance of the difference in means. The greater the absolute value of  $t$ , the less likely the two sample populations are taken from the same population.

A secondary output of the  $t$  test is the  $P$  value. This value is the normalized confidence probability, under the null hypothesis, of observing the difference given that the samples are taken from the same

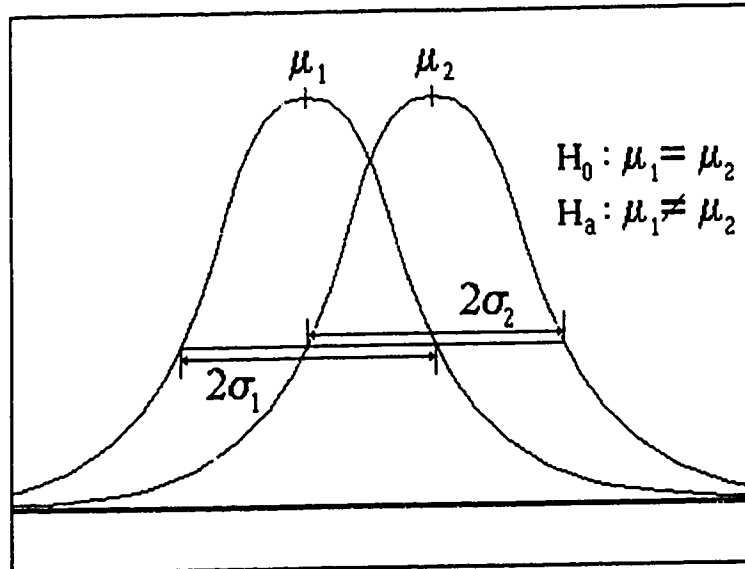


**Figure 2.2.** The  $t$  test measures the significance of the difference of the means of two populations.

population. For example, if the  $P$  value is 0.01, the probability of the null hypothesis is 1%. *The goal of this portion of the statistical study will be to reject the null hypothesis.*

In this study,  $t$  tests will be conducted by first dividing the data into two populations: days with lightning occurrence and days with no lightning occurrence. Each of the upper air parameters will be tested and results will then be surveyed to note the parameters that reject the null hypothesis. This will suggest that they are useful for distinguishing days with lightning from days without lightning.

It is worth noting two points about the  $t$  test. First, an important requirement for the  $t$  test is that the two sample populations must approximate a normal



distribution. Although no parameter has a true normal distribution, most approximate normality when sample sizes are large. Yet, some parameters clearly are not normally distributed. These are the previous day's flash total, dew-point depressions, and the wind directions. Both the previous day's flash totals and the dew-point depressions are limited to positive values and distributions are skewed with a large population at or near a value of zero. Wind directions have a wrap-around range where 0 and 360 degrees are equal. This is inappropriate for a normal distribution. Although the results from these variables are questionable, they remain in the study for completeness. Second, the  $t$  tests results do not correspond to our goal of separating the populations -- the test merely tells whether the observed differences in the samples can be expected from the same population. The results do give a good indication, however, of the relative importance of variables in the study.

#### **b. Logistic Regression**

Logistic regression is a method of regression analysis used on logical (true or false) data. The analysis predicts the occurrence of an event as a probability. The logistic regression is a curvilinear regression using the logistic response function described by the equation

$$E(U) = \frac{e^U}{1+e^U} \quad (2.13)$$

where  $E(U)$  is the predicted portion of successes (0 to 1).  $U$  is a linear function of one or more of the predictor variables of the form

$$U = a_1x_1 + a_2x_2 + \dots + a_nx_n + b \quad (2.14)$$

The logistic response function takes on a slanted "S" shape as shown in Figure 2.3. Models built using logistic regression give the probability of the predictand occurring. With a successful

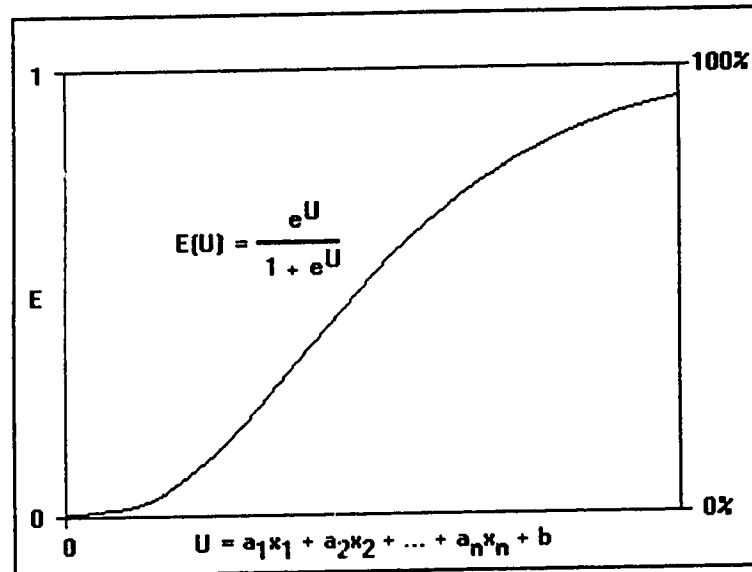


Figure 2.3. The logistic regression curve.

combination of predictors, the slope of the logistic response function will be steep, making predictions very reliable.

In this study, the technique will be used to predict the probability of lightning occurrence. Two models will be built. Model 1 will use variables chosen in a stepwise fashion. Stepwise regression is an iterative technique where predictors are added or removed one at a time to improve the overall goodness of fit of the regression. Model 2 will use selected variables. The choice of variables for Model 2 will be based on results from the  $t$  tests and on meteorological principles.

Skill scores will be used to assess the performance of the models and for verification. Skill scores measure the success and failure rates of predictions by comparing them with observations. Since the logistic models produce probabilities, the cut-off values must be chosen to discriminate between lightning and non-lightning occurrence. Cut-off values can be chosen anywhere between 0% and 100%, though the ideal cut-off value should be 50%. Actual cut-off values will be chosen to optimize skill score results.

The standard skill score measurements are the detection rate ( $P_d$ ), the false alarm rate ( $P_f$ ), and the critical success index ( $P_{si}$ ), all measured in percentages. For this thesis, the skill scores are defined as

$$P_d = 100\% \times \frac{\textit{correct lightning occurrence predictions}}{\textit{lightning occurrence observations}} \quad (2.15)$$

$$P_f = 100\% \times \frac{\textit{incorrect lightning occurrence predictions}}{\textit{lightning occurrence predictions}} \quad (2.16)$$

$$P_{si} = 100\% \times \frac{\textit{correct lightning occurrence predictions}}{\textit{lightning occurrence observations} + \textit{incorrect lightning occurrence predictions}} \quad (2.17)$$

In addition, a skill score measuring the total correct predictions of lightning occurrences and non-occurrences ( $P_{cor}$ ), designed by the author, has been included for comparative purposes.

$$P_{cor} = 100\% \times \frac{\text{correct lightning occurrence predictions} + \text{correct non-occurrence predictions}}{\text{total number of observations}} \quad (2.18)$$

### c. Linear Regression

Linear regression is a regression technique that attempts to predict values of a dependent variable with an independent variable using a linear correlation. The ability of the independent variable to explain the variation of the dependent is measured with the correlation coefficient  $r^2$ . The significance of the correlation is measured by  $P$ . In this study, linear regression will be used to assess the ability of each upper air parameter at predicting lightning frequency.

### d. Multiple Linear Regression

Multiple linear regression is a regression technique that produces a predictive equation using a linear combination of predictors. Stepwise linear regression is an iterative technique that attempts to find the best fit multiple linear regression from a list of potential predictors. Predictors are added or removed one at a time to improve the  $r^2$  value in a stepwise manner. Final coefficients of all variables will be

obtained by running a multiple linear regression using the predictors selected from the stepwise technique.

Three multiple linear regression models will be built to predict lightning flash frequency. Model 1 will use all days of data. Model 2 will use data for days when lightning occurred. Model 3 will use the logarithm of lightning flash frequency as the predictand, restricting its data to days when lightning occurred.

To verify the multiple linear regression models, lightning frequencies will be predicted for the independent 1988 data set. Predicted frequencies will be matched with those observed and compared using a paired  $t$  test to determine confidence limits for the models.

## **2.5 The Map Study**

The goal of the map study is to produce and verify spatial predictions of lightning occurrence and frequency over Alberta. The composite map study will introduce features that cannot be derived from a single upper air sounding. By assessing the importance of these parameters for predicting areas of intense lightning, the prediction models can be adjusted to produce a better forecast. The case study will be used to verify spatial interpolations based on the regression models produced in the statistical study and to justify the need to include composite map features.

**a. Composite Map Study**

The severe weather composite maps drawn by the forecasters at the severe weather desk of the Alberta Weather Centre in Edmonton will be studied. Composite maps were first introduced by Robert Miller (1967) as part of a technique to forecast severe weather.

Parameter	Symbol	Contribution
Surface		
Fronts		Lift
Moisture axis		Instability
Dry line		Instability
Thermal ridge		Instability
Convergence		Lift
Instability line		Instability
850 mb		
Axis of stronger wind		Lift
Low level jet		Lift
Moisture axis		Instability
Dry line		Instability
Thermal ridge		Instability
Convergence		Lift
700 mb		
Axis of stronger wind		Lift
Dry prod		Instability
No change line		Instability
Diffluent zones		Lift
500 mb		
Axis of stronger wind		Lift
Wind maximum		Lift
Thermal trough		Instability
PVA		Lift
Diffluent zones		Lift
250 mb		
Axis of stronger wind		Lift
Wind maximum		Lift
Diffluent zones		Lift
850-500 mb thickness ridge		Lift

**Figure 2.4.** Alberta Weather Centre's severe weather parameters and symbols.

In 1967, Miller wrote the United States Air Force manual on severe weather forecasting techniques that has stood as the standard reference. Miller's technique stresses the composite map. This map shows the most important features from all altitude levels that lead to instability or lift. Miller also rates the features according to their importance -- starting with positive vorticity advection (PVA) and continuing. Figure 2.4 shows the parameters emphasized by the severe weather forecasters at the Alberta

Weather Centre, their composite map symbols and their contribution to vertical velocities.

One must realize that Miller's techniques are used mainly to forecast severe thunderstorms and tornados. Lightning is more frequent and widespread than these phenomena and the success of this technique will be in the rejection or adoption of rules to find the features most important in forecasting areas of intense lightning.

The composite map study will be conducted primarily on a subjective basis. The patterns on composite maps will be compared with lightning maps. Each parameter on one day's composite map will be compared with the lightning flashes that occur for the same day. The comparison will be judged subjectively by assigning a value of 0 to 9 for the parameter's apparent contribution to the day's lightning. The assigned values and their descriptions are listed in Table 2.4.

Each parameter will be considered independently and locally. The possibility of parameter combinations leading to lightning will not be considered. Positional effects such as lightning upwind or downwind of a feature or to the left or right side will not be considered either. Results from this study will be compared to the parameters included in the statistical models. Those not covered will be used to adjust any spatial interpolations based on the statistical models.

**Table 2.4. Assigned values and descriptions for parameter contribution to lightning.**

Value	Description
0	Parameter absent
1	No contribution
2	No apparent contribution
3	No significant contribution
4	Possible contribution
5	No definite contribution
6	Marginal contribution
7	Significant contribution
8	Very significant contribution
9	Most significant contributor

**b. Case Study**

Spatial forecasts of lightning occurrence and frequency can be produced using the regression models from the statistical study and interpolated upper air fields as predictors. To illustrate this, the weighted moving averages technique is used. This technique interpolates values as

$$x' = \frac{\sum_{i=1}^n x_i/d_i^2}{\sum_{i=1}^n 1/d_i^2} \tag{2.19}$$

where  $x'$  is the interpolated value,  $x_i$  are the station values and  $d_i$  are the distances from the interpolation point to the observation stations. The station values are



weighted by one over the distance squared to emphasize the importance of close observations over those farther away.

The weighted moving averages is a simple technique that requires a minimal number of calculations. It does not require a first guess field and calculates values in one iteration. Its weaknesses are that it does not interpolate peak values in excess of the highest observed value and that it averages the results when extrapolating outside the observation network. The weighted moving averages scheme is a valid scheme to interpolate fire weather indices (Flannigan and Wotton 1989) and has been used successfully in fire management systems (Lee and Anderson 1990). Although there are more sophisticated techniques that emphasize meteorological processes, the weighted moving averages is adequate to illustrate the point.

In the case study, spatial prediction maps will be compared with actual lightning events recorded by the AFS's lightning detection system for four days from June 22 to 25, 1988. Results from the composite map study will be considered to determine if adjustments are required. The case study will evaluate the practicality of all the methods in this thesis.

## CHAPTER 3

### STATISTICAL STUDY OF LIGHTNING OCCURRENCE AND FREQUENCY

#### 3.1 Introduction

The goal of the statistical study of the lightning frequency is twofold. The first is to derive regression equations to predict lightning occurrence. The second goal is to derive regression equations to predict lightning frequency.

#### 3.2 Occurrence and Non-occurrence of Lightning

The first objective is to predict the probability of lightning occurrence. The statistical analyses used in the study to distinguish between days with lightning and days without lightning are the  $t$  test and logistic regression.

##### a. $t$ Test

In this portion of the study, each predictor parameter will be tested to see if it rejects the null hypothesis that the sample populations of days with lightning and days without lightning are from the same population. Those predictors that reject the null hypothesis will be considered significant in distinguishing between days with lightning and days without lightning.

Table 3.1 summarizes the  $t$  and  $P$  values for the four data sets. The table also shows the differences between morning (12:00 UTC) and afternoon (00:00 UTC)  $t$

values. A positive  $t$  value indicates that the predictor has a higher mean value for days with lightning than for days without. For the purpose of this study, a  $P$  value listed as 0.0000, which is actually less than 0.00005, will be a rejection of the null hypothesis.

The consistent importance of some variables is readily seen in both time periods and both polarities. Some variables are shown to be more significant at one time over the other, as indicated by a larger difference between the 12:00 UTC and the 00:00 UTC  $t$  values. The best indicators of lightning occurrence are the convective indices, emphasizing the convective nature of lightning. The best results are for the afternoon (00:00 UTC) George's K index with a  $t$  value of 9.55 for both the positive and the negative lightning occurrences.

The George's K index, cross totals, and total totals are more significant in the afternoon. The simplified K index, the lifted, and Showalter indices have little time preference.

Table 3.1. *t* test results for days with lightning versus days without lightning.

Parameter	1200 UTC				0000 UTC				<i>t</i> (0000 UTC) - <i>t</i> (1200 UTC)	
	Positive		Negative		Positive		Negative		Positive	Negative
	<i>t</i>	<i>P</i>	<i>t</i>	<i>P</i>	<i>t</i>	<i>P</i>	<i>t</i>	<i>P</i>		
PTOT2	1.32	0.1893	1.03	0.3023	1.35	0.1784	1.06	0.2885	0.03	0.03
NTOT2	1.52	0.1311	1.49	0.1378	1.55	0.1226	1.53	0.1284	0.03	0.04
WBZ	5.92*	0.0000	6.46*	0.0000	4.33*	0.0000	5.15*	0.0000	-1.59	-1.31
SfcPr	-2.14	0.0332	-2.18	0.0302	-2.98	0.0032	-3.09	0.0022	-0.84	-0.91
MSLP <sub>r</sub>	-3.02	0.0028	-3.20	0.0016	-3.17	0.0018	-3.30	0.0011	-0.15	-0.10
ZS	-2.95	0.0036	-3.11	0.0021	-3.23	0.0014	-3.36	0.0009	-0.28	-0.25
Z8	-1.06	0.2904	-0.97	0.3340	-2.44	0.0157	-2.50	0.0131	-1.38	-1.53
Z7	1.04	0.2977	1.42	0.1557	-0.88	0.3820	-0.65	0.5158	-1.92	-2.07**
Z5	2.07	0.0397	2.45	0.0149	-0.07	0.9467	0.32	0.7510	-2.14**	-2.13**
TS	5.18*	0.0000	5.71*	0.0000	0.75	0.4558	0.99	0.3223	-4.43**	-4.72**
T8	4.76*	0.0000	5.22*	0.0000	2.14	0.0335	2.26	0.0245	-2.62**	-2.96**
T7	3.95	0.0001	4.66*	0.0000	2.50	0.0131	2.93	0.0037	-1.45	-1.73
T5	2.23	0.0267	2.29	0.0231	0.09	0.9291	0.61	0.5414	-2.14**	-1.68
Td5	5.63*	0.0000	5.88*	0.0000	6.79*	0.0000	6.73*	0.0000	1.16	0.85
Td8	5.34*	0.0000	5.78*	0.0000	6.39*	0.0000	7.34*	0.0000	1.05	1.56
Td7	5.24*	0.0000	5.71*	0.0000	6.17*	0.0000	6.66*	0.0000	0.93	0.95
Td5	0.67	0.5019	1.18	0.2396	0.79	0.4294	1.19	0.2334	0.12	0.01
DDS	-1.32	0.1886	-0.79	0.4316	-5.15*	0.0000	-4.88*	0.0000	-3.83**	-4.09**
DD8	-0.53	0.5934	-0.50	0.6184	-3.88	0.0001	-4.40*	0.0000	-3.35**	-3.90**
DD7	-2.08	0.0385	-2.29	0.0226	-3.53	0.0005	-3.75	0.0002	-1.45	-1.46
DD5	0.63	0.5304	0.15	0.8808	-0.84	0.4047	-0.92	0.3576	-1.47	-1.07
F8	-2.23	0.0268	-1.75	0.0809	0.39	0.6949	0.60	0.5495	2.62**	2.35**
F7	-3.65	0.0003	-5.04*	0.0000	-1.05	0.2944	-0.97	0.3349	2.60**	4.07**
F5	-3.13	0.0020	-3.53	0.0005	-2.43	0.0157	-3.26	0.0013	0.70	0.27
TH8	-1.76	0.0806	-0.87	0.3834	0.89	0.3732	0.98	0.3260	2.65**	1.85
TH7	0.16	0.8753	-0.59	0.5549	-1.04	0.3002	0.02	0.9806	-1.20	0.61
TH5	-1.62	0.1068	-1.39	0.1671	-0.96	0.3366	-0.11	0.8971	0.66	1.26
dPR	-3.53	0.0005	-4.15*	0.0000	-2.95	0.0035	-3.31	0.0011	0.58	0.84
dZS	-3.73	0.0002	-4.24*	0.0000	-2.23	0.0267	-2.40	0.0172	1.50	1.84
dZ8	-3.15	0.0019	-3.95	0.0001	-3.52	0.0005	-4.09	0.0001	-0.37	-0.14
dZ7	-1.79	0.0745	-2.69	0.0076	-4.00	0.0001	-4.78*	0.0000	-2.21**	-2.09**
dZ5	-0.86	0.3915	-1.56	0.1203	-4.48*	0.0000	-4.99*	0.0000	-3.62**	-3.43**
dTS	3.04	0.0027	2.45	0.0149	-2.78	0.0061	-3.44	0.0007	-5.82**	-5.89**
dT8	2.73	0.0069	1.96	0.0513	-1.48	0.1412	-2.12	0.0349	-4.21**	-4.08**
dT7	2.60	0.0100	2.25	0.0251	-1.22	0.2235	-1.22	0.2238	-3.82**	-3.47**
dT5	0.12	0.9069	0.04	0.9681	-3.68	0.0003	-3.59	0.0004	-3.80**	-3.63**
TWS	6.05*	0.0000	6.40*	0.0000	4.31*	0.0000	4.59*	0.0000	-1.74	-1.81
TW8	6.01*	0.0000	6.49*	0.0000	4.82*	0.0000	5.54*	0.0000	-1.19	-0.95
WSR7	-3.00	0.0030	-4.08	0.0001	-1.13	0.2591	-0.59	0.5529	1.87	3.49**
WS75	-1.18	0.2397	-2.75	0.0064	-0.03	0.9725	-0.57	0.5672	1.15	2.18**
T87adv	0.69	0.4898	0.83	0.4049	-1.07	0.2857	-0.83	0.4090	-1.76	-1.66
T75adv	0.07	0.9422	0.42	0.6781	0.05	0.9634	0.15	0.8820	-0.02	-0.27
TH	4.19*	0.0000	4.68*	0.0000	2.00	0.0463	2.35	0.0197	-2.19**	-2.33**
dTH	2.33	0.0205	1.91	0.0572	-2.24	0.0261	-2.44	0.0155	-4.57**	-4.35**
K	6.46*	0.0000	6.84*	0.0000	9.55*	0.0000	9.55*	0.0000	3.09**	2.71**
K2	7.29*	0.0000	8.00*	0.0000	7.83*	0.0000	8.15*	0.0000	0.54	0.15
VT	4.28*	0.0000	4.84*	0.0000	3.09	0.0022	2.47	0.0143	-1.19	-2.37**
CT	3.92	0.0001	4.31*	0.0000	8.42*	0.0000	8.45*	0.0000	4.50**	4.14**
TT	5.60*	0.0000	6.20*	0.0000	8.62*	0.0000	8.23*	0.0000	3.02**	2.03**
SI	-6.86*	0.0000	-7.46*	0.0000	-8.67*	0.0000	-8.77*	0.0000	-1.81	-1.31
LI	-6.62*	0.0000	-6.98*	0.0000	-7.54*	0.0000	-7.02*	0.0000	-0.92	-0.04
Q	1.77	0.0782	2.02*	0.0446	1.88	0.0617	2.08	0.0390	0.11	0.06

\* indicates a greater than 99.995% confidence in the rejection of the null hypothesis.  
 \*\* indicates a difference in *t* values > 2.00 or < -2.00 between morning (12:00 UTC) and afternoon (00:00 UTC) soundings.

Moisture availability is important to convective activity and this is shown by the significance of the dew-point temperatures at levels below 500 mb. The dew-

point temperatures do show a time preference that is consistent at the three levels (surface, 850 mb, and 700 mb). The results for the wet-bulb temperatures show the importance of moisture as well, but due to the diurnal trend in the dry-bulb temperature discussed in the next paragraph, the afternoon  $t$  values are less significant than the morning values.

The dry-bulb temperature shows more significance in the morning sounding (12:00 UTC) than in the afternoon (00:00 UTC) when lightning is generally occurring. Also, the diurnal difference is most pronounced at the surface and steadily decreases with height. An explanation for the greater significance of the morning values over the afternoon values is probably the presence of moisture. The 12:00 UTC surface temperature usually represents close to the minimum temperature of the day. A warm minimum temperature could be due to a very warm air mass, a cloud cover insulating the lower atmosphere, or the latent heat released due to moisture -- all showing the presence of moisture. Contrarily, a high afternoon temperature does not show the presence or absence of moisture so does not distinguish between a hot, dry day with no convection and a hot, muggy day with much severe weather. Furthermore, thunderstorms before 00:00 UTC can cause severe drops in temperature. This also explains the low afternoon vertical totals values.

The dew-point depressions show a significant difference between the morning and afternoon values. This supports the argument concerning the poorer significance of the afternoon dry-bulb temperature. Here, the afternoon moisture is directly observed. The relative insignificance of the morning values can be explained by the overnight cooling trend that occurs every night. As the dry-bulb temperature falls and approaches the relatively static dew-point temperature, the dew-point depression drops to near zero. An event that occurs every night would naturally be a poor forecasting tool. Note that the values for the dew-point depression should be considered with caution as dew-point depressions are not normally distributed.

The wet-bulb zero proved to be significant in all cases. The positive  $t$  value indicates that the mean wet-bulb zero height is higher for days with lightning. A closer examination of the mean values indicates that for days with lightning, the mean altitude was about 2000 m (6000 ft.), while for days without lightning, the mean altitude was between 1500 and 1700 m (4500 to 5000 ft.). This agrees well with Miller's lower threshold or 1500 ft. for severe weather activity (1967). It would appear from the data that, in Alberta, the wet-bulb zero does not often reach Miller's upper threshold of 11,000 ft. for severe weather.

The 24-hour height changes for the afternoon show some significance that increases with height. This agrees with studies associating 500 mb height falls, showing the passage of an upper trough, with lightning fire ignitions (Janz and

Nimchuk 1985; Nimchuk 1983). Yet, the morning height falls show decreasing significance with height. The 00:00 UTC 500 mb height changes shows a significant distinction between days with lightning and days without lightning days ( $t$  values of -4.48 and -4.99 for positive and negative occurrences respectively) while the 12:00 UTC values are insignificant (-0.86 and -1.56). The lesser significance of the morning values can be attributed to a building ridge likely to follow a trough before the period of peak lightning activity.

Though expected to play a significant role, the 24-hour changes in pressure, temperature, and thickness performed poorly. A possible explanation for the poor results is that the scale is wrong. Twenty-four hour changes are too large to appreciate the motions of fronts and pressure systems. These parameters may serve as better predictors if measured hourly.

Curiously, morning wind speeds appear to have some influence on lightning occurrence with the most significant  $t$  value of -5.04 at 700 mb for negative lightning occurrence. In comparison, the afternoon soundings were relatively insignificant. The sign of the  $t$  value implies that lightning is more likely to occur at lower 700 mb wind speeds. A possible explanation for this may be turbulent mixing. In the morning, high mid-level wind could mix the atmosphere and disrupt any nocturnal inversion layer. This would greatly reduce the likelihood of intense convection later

in the day. Afternoon winds would play less of a role as thunderstorm development would have already begun.

#### **b. Logistic Regression**

In this study, logistic regression has been used to predict the probability of lightning occurrence. Two models were built. Model 1 used variables chosen in a stepwise fashion, while Model 2 used selected variables. The choice of variables for Model 2 were based on results from the *t* tests and on meteorological principles. The George's K and the simplified K Indices were chosen to represent the convective instability process. Low-level moisture was shown with the surface dew-point temperature. The wet-bulb zero height was used to represent the freezing level. The previous day's lightning flash total was included as a measure of persistence. For the 12:00 UTC sounding, the following additional predictors were included. The radiation term, *Q*, was chosen for the surface heating term. The temperature advection between 850 mb and 700 mb was used to show low-level warming and the temperature advection between 700 mb and 500 mb was used to show cooling aloft. These two predictors were excluded from the 00:00 UTC predictors because of their lower 00:00 UTC *t* test results. Presumably, their modifying effects are after-the-fact and will have little impact on convection. For the 00:00 UTC (afternoon) sounding, the 24-hour 500 mb height fall was included as an additional predictor.



Tables 3.2 and 3.3 show the variables entered in Models 1 and 2, their improvement  $P$  values, and the overall goodness of fit  $P$  value.

**Table 3.2. Model 1: logistic regression of days with lightning versus days with no lightning.**

Time	Polarity	Step	Variable	Improvement P	Goodness of fit P	Final Coefficient	
12:00	Positive	0	Constant		0.000	1.9005	
		1	K2	0.000	0.042	+0.10450	
		2	LI	0.040	0.055	-0.18010	
		3	dT8	0.015	0.083	+0.98254E-01	
	4	Q	0.057	0.101	+1.5872		
	Negative	0	Constant		0.000	0.000	-7.8675
1		K2	0.000	0.053	+0.21892		
2		Q	0.019	0.077	+1.8670		
00:00	Positive	0	Constant		0.000	-4.1628	
		1	K	0.000	0.376	+0.16015	
		2	SI	0.001	0.569	-0.12481	
		3	dTS	0.002	0.719	-0.33193	
		4	dT8	0.051	0.763	+0.23314	
	5	LI	0.097	0.789	-0.18910		
	Negative	0	Constant		0.000	0.000	-8.6033
		1	K	0.000	0.342	+0.14347	
		2	dZ5	0.001	0.528	-0.87183E-02	
		3	K2	0.001	0.693	+0.22958	
4		TS	0.039	0.746	-0.10536		

**Table 3.3. Model 2: logistic regression of days with lightning versus days with no lightning.**

Time	Polarity	Step	Variable	Improvement P	Goodness of fit P	Final Coefficient	
12:00	Positive	0	Constant		0.000	-7.0320	
		1	K2	0.000	0.039	+0.17850	
		2	Q	0.057	0.049	+1.5425	
		3	T87adv	0.602	0.046	+0.14700	
		4	TDS	0.731	0.042	+0.18953E-01	
		5	T75adv	0.892	0.038	+0.46430E-01	
		6	PTOT2	0.945	0.035	+0.31867E-03	
	7	WBZ	0.969	0.031	-0.18390E-04		
	Negative	0	Constant		0.000	0.000	-7.9750
		1	K2	0.000	0.050	+0.22242	
		2	Q	0.023	0.070	+1.8382	
		3	T87adv	0.506	0.067	+0.20801	
		4	T75adv	0.622	0.062	+0.14782	
		5	TdS	0.725	0.057	-0.25895E-01	
6		WBZ	0.727	0.053	+0.13771E-03		
7	NTOT2	0.830	0.045	-0.88148E-04			
00:00	Positive	0	Constant		0.000	-5.7064	
		1	K	0.000	0.369	+0.19443	
		2	dZS	0.004	0.503	-0.85208E-02	
		3	TdS	0.011	0.604	+0.11876	
		4	PTOT2	0.491	0.594	-0.42495E-02	
	5	WBZ	0.582	0.582	-0.22787E-03		
	Negative	0	Constant		0.000	0.000	-5.8992
		1	K	0.000	0.322	+0.20351	
		2	dZS	0.001	0.500	-0.10325E-01	
		3	TdS	0.019	0.583	+0.80372E-01	
4		NTOT2	0.360	0.580	-0.42561E-03		
5	WBZ	0.502	0.570	+0.26837E-03			

For Model 1, the most significant variable for both polarities and both time periods is a convective index (K2 and K). This conforms with *t* test results, where convective indices were the most significant. In more general terms, the model shows that convective instability is the most important process in predicting lightning occurrence. The second and following steps enter a variety of variables. The radiation term, the 24-hour temperature changes at the surface and at 850 mb, and the surface temperature indicate surface heating. The 24-hour 500 mb height

changes indicate the passage of an upper level trough. The lifted and the Showalter indices support the importance of convection.

For Model 2, the chosen variables were forced into the model. In doing so, the entry of some variables was relatively insignificant (high improvement  $P$  values) and, to a small degree, reduced the overall goodness of fit of the model. Yet, to limit the entry of variables to low  $P$  values, as was done in Model 1, would result in almost the same variables as those in Model 1. Because of this, the results from both models may be very similar.

Table 3.4 summarizes the skill scores for the prediction of lightning occurrence using the 1986 and 1987 data with cut-off points maximized for the  $P_{si}$  (critical success index). Cut-off points ranged from 27.5% to 55.8%. On this table, the  $P_d$  (detection rate) from 78.02% to 97.44%, the  $P_f$  (false alarm rate) from 17.70% to 43.24%, and the  $P_{si}$  ranges from 53.50% to 67.39%. These can be considered very good prediction results though some false alarm rates are a concern. As seen from the low cut-off points, the logistic regression has not handled the discrimination point well. This is because logistic regression is not designed to test for these kinds of scores but more for the  $P_{cor}$  (percent correctly predicted) value, which ranges from 69.33% to 81.09%.

**Table 3.4. Skill scores for the logistic regression models.**

Model	Time	Polarity	Cut	A	B	C	D	$P_d$	$P_f$	$P_{si}$	$P_{cor}$
1	12:00	Positive	0.358	80	14	55	91	85.11	40.74	53.69	71.25
		Negative	0.475	97	22	35	88	81.51	26.52	62.99	76.45
	00:00	Positive	0.392	77	16	31	115	82.80	28.70	62.10	80.33
		Negative	0.558	93	25	20	100	78.81	17.70	67.39	81.09
2	12:00	Positive	0.308	84	9	64	81	90.32	43.24	53.50	69.33
		Negative	0.425	103	15	47	73	87.29	31.33	62.42	73.95
	00:00	Positive	0.408	71	20	32	113	78.02	31.07	57.72	77.97
		Negative	0.275	114	3	56	63	97.44	32.94	65.90	75.00

A = lightning forecasted and observed  
 B = lightning not forecasted but observed  
 C = lightning forecasted but not observed  
 D = lightning not forecasted and not observed  
 $P_d = 100\% \times A/(A+B)$  "probability of detection"  
 $P_f = 100\% \times C/(A+C)$  "probability of false alarm"  
 $P_{si} = 100\% \times A/(A+B+C)$  "critical success index"  
 $P_{cor} = 100\% \times (A+D)/(A+B+C+D)$  "percent correct"

The results show small differences between the models. Model 1 has the best  $P_{si}$  scores overall, though in most cases, the differences between corresponding predictions are only a small percentage. Model 2 has better detection rates, but also has high false alarm rates resulting in the somewhat poorer  $P_{si}$  scores noted above.

To verify the logistic regression models, the independent 1988 data were entered into the model equations to predict lightning occurrence. Predicted and observed results were tabulated as the skill scores shown in Table 3.5.

**Table 3.5. Skill scores for the verification of the logistic regression models.**

Model	Time	Polarity	Cut	A	B	C	D	$P_d$	$P_f$	$P_{si}$	$P_{cor}$
1	12:00	Positive	0.358	30	14	34	38	68.18	53.13	38.46	58.62
		Negative	0.475	41	21	25	32	66.13	37.88	47.13	61.34
	00:00	Positive	0.392	28	16	24	51	63.64	46.15	41.18	66.39
		Negative	0.558	39	23	19	38	62.90	32.76	48.15	64.71
2	12:00	Positive	0.308	31	10	38	31	75.61	55.07	39.24	56.36
		Negative	0.425	40	18	25	27	68.97	38.46	48.19	60.91
	00:00	Positive	0.408	32	12	24	50	72.73	42.86	47.06	69.49
		Negative	0.275	51	11	33	23	82.26	39.29	53.68	62.71

A = lightning forecasted and observed  
 B = lightning not forecasted but observed  
 C = lightning forecasted but not observed  
 D = lightning not forecasted and not observed  
 $P_d = 100\% \times A/(A+B)$  "probability of detection"  
 $P_f = 100\% \times C/(A+C)$  "probability of false alarm"  
 $P_{si} = 100\% \times A/(A+B+C)$  "critical success index"  
 $P_{cor} = 100\% \times (A+D)/(A+B+C+D)$  "percent correct"

Results from the verification conform well with those of the model. The skill scores for the verification are still good with  $P_{si}$  (critical success index) values ranging from 38.46% to 53.68%. The detection rate ( $P_d$ ) is high, the best results predicting more than 70% of the days with lightning. Yet, the high false alarm rates, as mentioned before, show the models have over-predicted lightning, such that as much as 55% of the lightning forecasts turned out to be for non-lightning days.

### 3.4 Frequency of Lightning Flashes

The second problem to be resolved is to predict lightning frequency. This will be accomplished through linear and multiple linear regression.

### a. Linear Regression

Table 3.6 presents the correlation coefficient ( $r$ ) values when a linear regression is calculated against the positive or negative flash frequencies. A survey of the  $r$  values show poor results. Excluding the correlation with previous days lightning values (which have a large number of points at the origin), the highest absolute value of 0.341 gives an  $r^2$  of 0.116 indicating that only 11.6% of the variation of lightning frequency is represented by the regression line. The  $P$  values indicate the probability that the correlation is due to chance. In several cases, the  $P$  value is less than 0.001. This indicates that, though these parameters may be poor predictors of lightning frequency, their correlation is not due to chance.

For 244 cases, a  $P$  value of 0.001 corresponds to an absolute  $r$  value of 0.22 ( $r^2$  of 0.0484). Parameters with absolute  $r$  values greater than this value include the wet-bulb zero height, the dry-bulb, wet-bulb, and dew-point temperatures at all levels, the 1000-500 mb thickness, and the convective indices -- with the exclusion of the vertical totals. There appears to be no significant differences in the correlations for the two time periods or for the two polarities, except for the convective indices. These showed better correlation for afternoon models in all cases.

**Table 3.6. Correlation coefficients for linear regressions of parameters against the number of lightning flashes.**

Parameter	1200 UTC Positive			1200 UTC Negative			0000 UTC Positive			0000 UTC Negative		
	r	N	P	r	N	P	r	N	P	r	N	P
PTOT2	0.313*	242	<0.001	0.215	242	0.001	0.313*	242	<0.001	0.215	242	<0.001
NTOT2	0.451*	242	<0.001	0.300*	242	<0.001	0.451*	242	<0.001	0.300*	242	<0.001
WBZ	0.269*	243	<0.001	0.273*	243	<0.001	0.278*	242	<0.001	0.320*	242	<0.001
SfcPr	-0.071	243	0.266	-0.019	243	0.773	-0.175	242	0.006	-0.122	242	0.056
mSLPr	-0.107	243	0.094	-0.061	243	0.339	-0.190	242	0.003	-0.153	242	0.017
ZS	-0.106	243	0.098	-0.058	243	0.364	-0.194	242	0.002	-0.155	242	0.015
Z8	-0.021	243	0.750	0.038	243	0.551	-0.135	242	0.034	-0.071	242	0.269
Z7	0.101	243	0.115	0.156	243	0.015	-0.013	241	0.838	0.057	241	0.377
Z5	0.169	243	0.008	0.211	243	<0.001	0.066	241	0.304	0.127	241	0.048
TS	0.197	243	0.002	0.222*	243	<0.001	0.068	242	0.288	0.129	242	0.045
T8	0.231*	242	<0.001	0.245*	242	<0.001	0.199	242	0.002	0.239*	242	<0.001
T7	0.271*	243	<0.001	0.284*	243	<0.001	0.214	241	<0.001	0.241*	241	<0.001
T5	0.175	243	0.006	0.178	243	0.005	0.131	241	0.042	0.144	241	0.024
TdS	0.270*	243	<0.001	0.266*	243	<0.001	0.265*	242	<0.001	0.282*	242	<0.001
Td8	0.289*	243	<0.001	0.268*	243	<0.001	0.288*	242	<0.001	0.321*	242	<0.001
Td7	0.176	243	0.006	0.166	243	0.009	0.264*	241	<0.001	0.275*	241	<0.001
Td5	-0.037	243	0.565	-0.061	243	0.340	0.023	241	0.721	0.084	241	0.194
DDS	-0.121	243	0.059	-0.085	243	0.187	-0.177	242	0.006	-0.139	242	0.029
DD8	-0.068	242	0.290	-0.034	242	0.596	-0.091	242	0.158	-0.086	242	0.182
DD7	0.021	243	0.742	0.042	243	0.051	-0.086	241	0.180	-0.076	241	0.241
DD5	0.154	243	0.015	0.184	243	0.004	0.063	241	0.329	0.004	241	0.945
F8	-0.092	241	0.152	-0.066	241	0.309	0.049	240	0.447	0.071	240	0.272
F7	-0.130	241	0.043	-0.128	241	0.046	0.051	240	0.429	-0.018	240	0.782
F5	-0.112	242	0.080	-0.139	242	0.030	0.017	240	0.788	-0.048	240	0.457
TH8	-0.180	241	0.005	-0.181	241	0.005	-0.165	240	0.010	-0.133	240	0.039
TH7	-0.037	241	0.563	-0.033	241	0.609	-0.134	240	0.037	-0.178	240	0.005
TH5	-0.128	242	0.045	-0.099	242	0.124	-0.127	240	0.048	-0.144	240	0.025
dPR	-0.098	242	0.128	-0.046	242	0.471	-0.203	240	0.001	-0.171	240	0.007
dZS	-0.096	242	0.135	-0.049	242	0.444	-0.180	240	0.005	-0.152	240	0.018
dZ8	-0.094	242	0.144	-0.041	242	0.523	-0.216	240	<0.001	-0.184	240	0.004
dZ7	-0.074	242	0.248	-0.036	242	0.581	-0.193	238	0.003	-0.159	238	0.014
dZ5	-0.065	242	0.315	-0.033	242	0.608	-0.170	238	0.008	-0.122	238	0.059
dTS	0.037	242	0.569	0.049	242	0.444	-0.069	240	0.286	-0.064	240	0.325
dT8	0.035	240	0.591	0.000	240	1.000	0.017	240	0.796	0.016	240	0.800
dT7	0.015	242	0.812	0.012	242	0.854	0.032	238	0.623	0.059	238	0.367
dT5	-0.027	242	0.677	-0.029	242	0.658	-0.117	238	0.072	-0.069	238	0.286
TWS	0.261*	243	<0.001	0.271*	243	<0.001	0.222*	242	<0.001	0.262*	242	<0.001
TW8	0.323*	242	<0.001	0.315*	242	<0.001	0.291*	242	<0.001	0.333*	242	<0.001
WS87	-0.069	241	0.283	-0.060	241	0.350	0.108	240	0.095	0.068	240	0.292
WS75	-0.150	241	0.019	-0.169	241	0.008	0.112	240	0.081	0.068	240	0.294
T87adv	0.085	241	0.188	0.093	241	0.150	0.029	240	0.634	0.030	240	0.648
T75adv	0.035	241	0.593	0.035	241	0.587	0.194	240	0.702	0.144	240	0.025
TH	0.245*	243	<0.001	0.259*	243	<0.001	0.188	241	0.003	0.224*	241	<0.001
dTH	0.018	242	0.777	0.010	242	0.882	-0.009	238	0.891	0.011	238	0.868
K	0.203	242	0.001	0.184	242	0.004	0.313*	241	<0.001	0.345*	241	<0.001
K2	0.318*	242	<0.001	0.310*	242	<0.001	0.330*	241	<0.001	0.382*	241	<0.001
VT	0.122	242	0.058	0.139	242	0.031	0.132	241	0.041	0.171	241	0.007
CT	0.170	243	0.008	0.142	243	0.026	0.224*	241	<0.001	0.250*	241	<0.001
TT	0.201	242	0.002	0.190	242	0.003	0.256*	241	<0.001	0.301*	241	<0.001
SI	-0.300*	242	<0.001	-0.282*	242	<0.001	-0.313*	241	<0.001	-0.362*	241	<0.001
LI	-0.194	243	0.002	-0.206*	243	0.002	-0.215	241	<0.001	-0.256*	241	<0.001
O	0.048	244	0.451	0.061	244	0.338	0.045	244	0.480	0.059	244	0.359

\*  $r > 0.220$  or  $r < -0.220$  indicate a greater than 99.9% confidence that the correlation is not due to chance.

Because of the low  $r$  values, it is hard to draw any firm conclusions from these results. One could conclude from the evidence that the results support the convective nature of lightning. In both positive and negative flash totals, the

significant variables are those that measure convective instability, available low-level moisture, and warm low-level temperatures.

#### **b. Multiple Linear Regression**

Three multiple linear regression models were built to predict lightning flash frequency. Model 1 used all days of data. Model 2 used data for days when lightning occurred. Model 3 used the logarithm of lightning flash frequency as the predictand, restricting its data to days when lightning occurred. The results of the models are shown in Tables 3.7, 3.8, and 3.9.

Table 3.7 shows the results for the stepwise linear regression using data for all days. In this case, the regression is attempting to predict days with no lightning (zero flashes) as well as the number of lightning flashes for days with lightning. The first predictor entered for both time periods and both polarities was the simplified K index. Further steps added a variety of new predictors that marginally increased the  $r^2$  values. Final  $r^2$  values were between 0.1115 and 0.3022.



**Table 3.7. Model 1: stepwise linear regression to predict the total number of flashes using data for days with lightning and days with no lightning.**

Time	Polarity	Step	Variable		$r^2$	Change in $r^2$	Final Coefficient	
			entered	removed				
12Z	Positive	0	Constant				-27.62170	
		1	K2		0.0945	0.0945	2.43135	
		2	Q		0.1034	0.0089	18.12367	
		3	T87adv		0.1119	0.0085	3.86571	
		4	K		0.1158	0.0039	-0.03749	
		5	dT5		0.1215	0.0056	-0.53430	
		6	TdS		0.1266	0.0051	1.23398	
		7	NTOT2		0.1315	0.0050	-0.00516	
		8	TS		0.1372	0.0057	-2.35554	
		9	CT		0.1532	0.0160	-1.73192	
		10		K		0.1527	-0.0004	
	11	dT8		0.1566	0.0039	-0.44897		
		Final		0.1567				
		Negative	0	Constant				-1779.03809
	1		K2		0.0752	0.0752	27.45158	
	2		T87adv		0.0841	0.0090	84.54250	
	3		Q		0.0926	0.0085	260.12988	
	4		K		0.1003	0.0077	-6.88374	
	5		dT8		0.1057	0.0055	-8.11655	
	6		Z8		0.1138	0.0081	0.72665	
	Final		0.1115					
00Z	Positive	0	Constant				10.60751	
		1	K2		0.1432	0.1432	8.05615	
		2	TS		0.1636	0.0204	-6.46085	
		3	CT		0.1757	0.0121	-6.88978	
		4	PTOT2		0.1839	0.0082	0.18505	
		5	Q		0.1897	0.0059	-0.56151	
		Final		0.3022				
		Negative	0	Constant				-114.38557
	1		K2		0.1461	0.1461	1.76327	
	2		dTS		0.1557	0.0096	-22.64159	
	3		dT8		0.1691	0.0135	21.55051	
	4		Q		0.1757	0.0066	147.69679	
	5		SI		0.1799	0.0042	-46.30862	
	6		LI		0.1914	0.0115	21.60083	
7	WBZ			0.1958	0.0045	0.06703		
8		K2		0.1958	0.0000			
9	ZS		0.2007	0.0049	0.43835			
	Final		0.1933					

**Table 3.8. Model 2: stepwise linear regression to predict the total number of lightning flashes using only data for days with lightning.**

Time	Polarity	Step	Variable		$r^2$	Change in $r^2$	Final coefficient
			entered	removed			
12Z	Positive	0	Constant				13.95103
		1	K2		0.1013	0.1013	-1.06880
		2	dTS		0.1192	0.0179	-2.62408
		3	T87adv		0.1423	0.0231	13.58185
		4	T8		0.1685	0.0262	2.73196
		5	SI		0.1792	0.0107	-4.19089
		6		K2	0.1785	-0.0008	
	7	Q		0.1925	0.0141	22.79721	
				0.1948			
	Negative	0	Constant				-4003.67578
		1	K2		0.0706	0.0706	52.16466
		2	T87adv		0.0858	0.0151	196.94600
		3	K		0.0982	0.0125	-16.30254
		4	dT8		0.1174	0.0191	-31.72899
5		Z8		0.1336	0.0162	1.81935	
6		Q		0.1530	0.0194	513.44507	
7	NTOT2		0.1613	0.0083	-0.17611		
	Final		0.1613				
00Z	Positive	0	Constant				-19.54021
		1	K2		0.1143	0.1143	6.25076
		2	LI		0.1480	0.0337	4.53442
		3	Z8		0.1656	0.0176	-0.09772
		4	T87adv		0.1902	0.0246	16.68277
		5	PTOT2		0.2052	0.0150	0.68108
		6	TS		0.2165	0.0113	-1.60976
		Final		0.4897			
	Negative	0	Constant				-5115.74609
		1	K2		0.1407	0.1407	84.30721
		2	dTS		0.1654	0.0247	-47.72008
		3	dT8		0.1934	0.0280	38.70982
		4	TdS		0.2063	0.0129	-22.06084
		5	K		0.2208	0.0145	14.33018
6		SI		0.2326	0.0118	138.73404	
7	TT		0.2422	0.0096	42.88992		
	Final		0.2389				

**Table 3.9. Model 3: stepwise linear regression to predict the logarithm of the total number of lightning flashes using only data for days with lightning.**

Time	Polarity	Step	Variable		$r^2$	Change in $r^2$	Final coefficient
			entered	removed			
12Z	Positive	0	Constant				-1.02258
		1	K2		0.0879	0.0879	0.04265
		2	Q		0.1251	0.0372	0.73117
		3	PTOT2		0.1494	0.0244	-0.33929E-03
		4	TdS		0.1780	0.0286	0.02978
		5	dZ5		0.1968	0.0188	-0.00132
		6	TS		0.2094	0.0126	-0.02355
	Final			0.1764			
	Negative	0	Constant				13.78446
		1	TdS		0.0507	0.0507	0.09431
		2	Q		0.0756	0.0249	1.17293
		3	SI		0.0983	0.0227	-0.45213
		4	TS		0.1087	0.0103	-0.18193
		5	CT		0.1177	0.0090	-0.03695
		6	dT5		0.1298	0.0121	-0.11014
		7	dTS		0.1599	0.0300	0.10806
		8	TT		0.1859	0.0260	-0.21215
		9		CT	0.1802	-0.0057	
	Final			0.2093			
00Z	Positive	0	Constant				-0.29499
		1	Td8		0.0718	0.0718	0.02927
		2	PTOT2		0.0987	0.0269	-0.00457
		3	Q		0.1256	0.0269	0.60553
		4	DZ5		0.1438	0.0182	-0.00190
		5	T87adv		0.1698	0.0260	0.32205
		6	K		0.1817	0.0119	0.01993
	Final			0.1817			
	Negative	0	Constant				-15.58356
		1	K		0.1301	0.1301	0.05661
		2	T75adv		0.1508	0.0208	-0.54520
		3	Q		0.1712	0.0203	0.69920
		4	TT		0.1909	0.0198	0.25543
		5	dTS		0.2008	0.0099	-0.15643
		6	dT8		0.2541	0.0533	0.16351
		7	PTOT2		0.2788	0.0247	0.01072
		8	WBZ		0.2858	0.0070	0.87305E-03
		9	SI		0.3263	0.0406	0.36608
		10	T87adv		0.3347	0.0083	0.25378
		Final			0.3224		

By using only days with lightning, Model 2 attempts to predict the number of lightning flashes under the assumption there will be lightning that day. The results are shown on Table 3.8. The  $r^2$  values were higher than those using data for all days. As in the previous study, the first predictor entered was the simplified K index. Again, further steps added a variety of new predictors that increased the  $r^2$  values marginally. Final  $r^2$  values were between 0.1613 and 0.4897.

The third model uses the base 10 logarithm of the number of lightning flashes for days with lightning. The results are summarized in Table 3.9. Unlike the previous models, a convective index was not always the first parameter added. The 12:00 UTC logarithm of the negative flash frequency added the surface dew-point temperature first and the 00:00 UTC logarithm of the positive flash frequency added the 850 mb dew-point temperature first. Also, the significance of the first step in three of the four regressions was not as strongly weighted when compared to the remaining steps. The overall results are very similar for the two time periods. Final  $r^2$  values range from 0.1764 to 0.3224.

A peculiarity of the equations shows the prediction of negative numbers of lightning flashes. Naturally, this is an impossibility but, if these values are interpreted as days with no lightning, there are few inconsistencies. This supports the results from the logistical regression analysis showing that the distinction between days with lightning and days with no lightning can be accurately determined.

To verify the multiple linear regression models, lightning frequencies were predicted using the independent 1988 data set. Predicted frequencies were matched with those observed and compared using a paired  $t$  test. Results are shown in Table 3.10.

**Table 3.10. Paired  $t$  test values of verification of multiple linear regression models.**

Model	Time	Polarity	$t$	P	Predicted - Observed		N
					Mean	St. D.	
1	12:00	Pos	1.44	0.1521	2.2377	16.0450	107
		Neg	2.86	0.0050	64.2637	233.1397	108
	00:00	Pos	1.57	0.1198	2.5585	17.8884	120
		Neg	3.42	0.0009	64.0569	203.5086	118
2	12:00	Pos	0.49	0.6251	1.9416	25.2495	41
		Neg	2.13	0.0377	105.0438	376.0342	58
	00:00	Pos	1.24	0.2224	5.9130	30.1595	40
		Neg	1.36	0.1775	58.3764	336.9248	62
3	12:00	Pos	-0.52	0.6064	-0.0479	0.6053	43
		Neg	2.38	0.0203	0.2763	0.9057	61
	00:00	Pos	-0.54	0.5932	-0.0492	0.5782	40
		Neg	-0.62	0.5377	-0.0900	1.1055	58

For Models 1 and 2, positive  $t$  values show on average an over-prediction of the number of lightning flashes.  $P$  values, which measure the probability under the

null hypothesis of observing the differences given that the predicted and observed lightning flash frequencies are from the sample population, vary considerably. Except for the 12:00 UTC negative flash regression, Model 3, predicting the logarithm of the flash frequency, did well with  $P$  values between 0.50 and 0.60. Model 1 did the worst with  $P$  values below 0.15. Curiously, the 12:00 UTC predictions of negative lightning flash frequency fared poorly in all three models, with a less than 5% confidence in the null hypothesis.

## CHAPTER 4

### MAP ANALYSIS OF AREAS OF INTENSE LIGHTNING

#### 4.1 Introduction

The goal of the map analysis study is to produce spatial predictions of lightning. This has been accomplished through the study of composite maps and the spatial interpolation of the regression models produced in the statistical study.

#### 4.2 Composite Map Study

Composite map features have been compared with areas of intense lightning activity to assess the importance each feature has in determining where lightning occurs. Table 4.1 summarizes the results. On this table, the parameters are listed with the mean, standard deviation, and the number of occurrences.

The first impression one gets from the data is that most mean values are below 5.0, showing a low contribution to lightning pattern. The low values are a result of averaging over the entire season. Quite often some features were present on days with little to no lightning and therefore received a value of one. Also, the intensity, or strength of a feature is not considered in this approach, arbitrarily pulling down the average.

**Table 4.1. Parameter significance summary.**

Level	Parameter	1986			1988			1989			Combined		
		Mean	St.D.	N	Mean	St.D.	N	Mean	St.D.	N	Mean	St.D.	N
Surface	Warm front	6.94*	1.82	17	na	na	0	na	na	0	6.94*	1.82	17**
	Cold front	5.75*	2.56	28	na	na	0	na	na	0	5.75*	2.56	28
	Moisture axis	6.44*	1.83	62	3.39	2.33	36	6.26*	1.59	69	5.71*	2.22	167
	Dry line	3.33	3.21	3**	na	na	1**	na	na	0	2.75	2.87	4**
	Thermal ridge	4.90	2.39	48	na	na	0	na	na	0	4.90	2.39	48
	Convergence	5.33*	2.08	3**	na	na	0	na	na	0	5.33*	2.08	3**
	Instability line	na	na	0	na	na	0	na	na	0	na	na	0
850 mb	Axis of stronger wind	4.11	2.20	36	3.46	1.61	13	4.58	1.98	24	4.15	2.05	73
	Low-level jet	2.33	1.53	3**	3.67	3.06	3**	na	na	0	3.00	na	na
	Moisture Axis	6.09*	2.01	80	4.35	2.24	31	5.94*	1.67	78	5.74*	2.01	169
	Dry line	5.13*	2.64	8**	na	na	1**	na	na	0	5.33*	2.55	9**
	Thermal ridge	5.29*	2.15	70	3.75	2.06	32	5.36*	2.06	66	5.02*	2.17	168
	Convergence	5.79*	2.46	33	4.90	2.60	10	na	na	1**	5.48*	2.56	44
700 mb	Axis of stronger wind	4.43	2.35	72	4.37	2.28	30	4.73	1.99	41	4.50	2.23	143
	Dry prod	4.40	0.89	5**	2.40	2.11	10	4.70	2.00	44	4.27	2.12	59
	No change line	3.83	2.11	71	3.76	2.05	17	na	na	0	3.82	2.09	88
	Diffluent zone	3.93	2.84	14	3.50	2.12	2**	na	na	0	3.88	2.70	16**
500 mb	Axis of stronger wind	3.52	2.47	62	4.41	2.34	27	5.00*	2.03	36	4.14	2.39	125
	Wind maximum	3.13	2.70	8**	4.00	2.20	8	4.50	2.65	4**	3.75	2.43	20
	Thermal trough	5.94*	2.00	50	3.48	2.04	25	5.50*	1.60	52	5.28*	2.06	127
	PVA	4.17	2.48	54	4.68	2.41	31	5.58*	1.86	45	4.78	2.33	130
	Diffluent zone	4.19	2.58	21	6.67*	1.53	3**	na	na	0	4.50	2.59	24
250 mb	Axis of stronger wind	3.84	2.21	50	4.35	2.35	26	4.78	1.97	49	4.32	2.18	125
	Wind maximum	4.50	2.12	2**	3.86	2.34	7	4.80	1.79	5**	4.29	2.02	14**
	Diffluent zone	4.00	2.55	21	5.25*	3.40	4**	na	na	1**	4.23	2.61	26
	PVA	na	na	0	4.20	2.27	15	4.89	1.92	46	4.72	2.02	61
1000 mb - 500 mb thickness Ridge		6.20*	1.90	15	4.93	2.46	14	na	na	0	5.59*	2.24	29
Total totals index > 50		na	na	0	5.25*	2.05	8	6.20*	1.47	59	6.09*	1.56	67

\* = a parameter with an average value of 5.00 or greater  
 \*\* = a frequency that was less than 10%

One must be careful considering results from features that were plotted infrequently. A high mean from a feature that was plotted only a few times may be biased due to its intensity or may have been an effect, rather than the cause, of the weather pattern.

A feature is considered significant if it has a mean value of 5.0 or greater and occurrences on 10% or more of the maps. The ranked list of significant features with their means and percent occurrences is shown in Table 4.2.



**Table 4.2. Ranked listing of significant features with more than 10% occurrence.**

Rank	Parameter	Mean Value	Percent Occurrence
1	Total totals index > 50	6.09	31.6
2	Surface cold front	5.75	13.2
3	850 mb moisture axis	5.74	89.2
4	Surface moisture axis	5.71	78.8
5	1000-500 mb thickness ridge	5.59	13.7
6	850 mb convergence	5.48	20.8
7	500 mb thermal trough	5.28	59.9
8	850 mb thermal ridge	5.02	79.2

The significance of low-level moisture, warm low-level temperature, and instability continue to emphasize the role of convection in lightning occurrence. These features were plotted more than half the days studied.

The 1000-500 mb thickness ridge and low-level convergence are shown to be the most important lifting parameters. Unfortunately, they were not plotted frequently and perhaps are not as good an indicator.

Positive vorticity advection at both 500 mb and 250 mb came close to meeting significance criteria with mean values of 4.78 and 4.72 respectively. Lower values could be attributed to a lack of consideration for the intensity of the advection.

Surface fronts must be considered with caution. In analyzing fronts, one important aspect the forecaster looks for is significant weather -- especially in analyzing warm fronts. In this respect, the cause and effect roles may be reversed. Also, during the years studied, the severe weather desk showed a varying commitment to including fronts on their composite maps. Results for the front could be considered with more confidence if they were included more often.

Comparing these results with those of the statistical models, several parameters are common. Moisture, temperature, and instability are included in the regression equations. It can also be argued that the 1000-500 mb thickness ridge is represented by the 500 mb height falls as it moves out of the forecast region. When the equations are interpreted spatially, these features are accounted for. Features that are not covered include fronts, low-level convergence, and PVA. These will be the features that must be considered to adjust any spatial prediction models.

### **4.3 A Case Study**

To validate the methods in this thesis, a case study is used. The study covers a four-day period from June 22 to 25, 1988. Lightning activity during this period went from little on the first day to intense on the second and third. On the fourth day, the activity dropped again. Lightning detection maps for these four days are shown in Figures 4.1 to 4.4. The daily lightning counts picked up by the LLP system were 297, 4375, 5437, and 369.

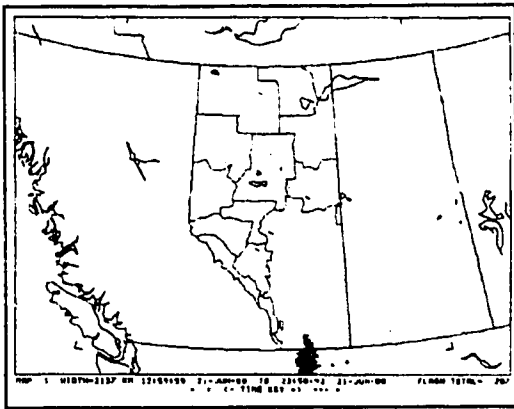


**Figure 4.1.** Lightning detection map for June 21, 1988.

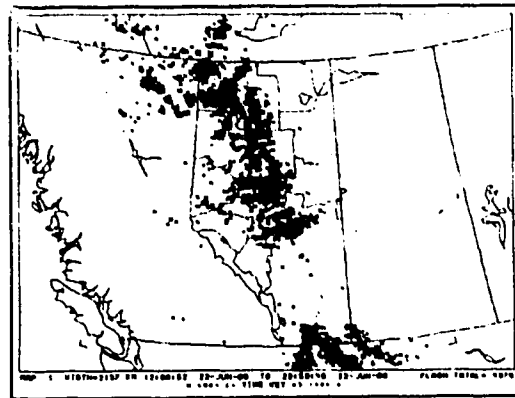


**Figure 4.2.** Lightning detection map for June 22, 1988.

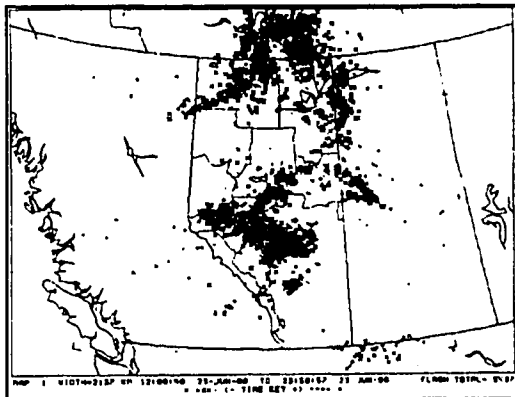


**Figure 4.3.** Lightning detection map for June 23, 1988.

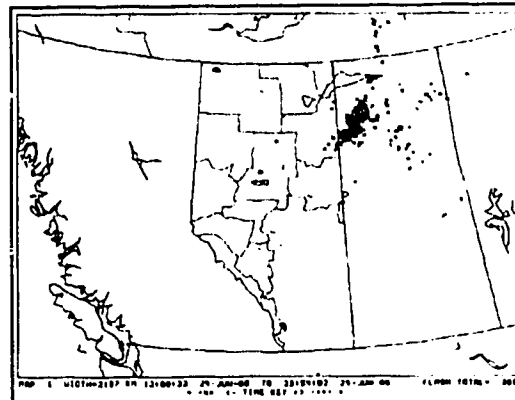


**Figure 4.4.** Lightning detection map for June 24, 1988.

The two active days were of particular interest because on each of these days, two distinct areas of lightning activity occurred. June 22 saw a broad band of lightning activity from Edmonton northwest through to High Level where the pattern dispersed. A second storm occurred in a tight pattern along the southern Alberta border. June 23 saw renewed lightning activity over central Alberta stretching from Hinton to east of the Alberta-Saskatchewan border while a second area occurred in

the northeast, centered around Fort Smith. Over the four-day period, the 500 mb flow was primarily zonal. A ridge left Alberta on June 22 creating a southwesterly flow that flattened out by June 24. A series of short waves moved along the flow with negligible vorticity advections. One strong vorticity centre moving along the southwesterly flow in the wake of the ridge brought significant PVA (positive vorticity advection) over most of central and southern Alberta during the evening of June 22 (June 23 UTC). A second vorticity centre moved rapidly across Alberta between 00:00 UTC and 12:00 UTC on June 24.

The surface pattern began with a high pressure system over central Alberta and a stationary front near the southern Alberta border. At 0600 UTC on June 22 a low formed in the lee of the Rockies 100 km north of Jasper. A TROWAL (trough of warm air aloft) extended northwestward from the low as it moved eastward into Alberta. The low and TROWAL moved slowly across Alberta, bringing clouds to most of Alberta for the next 24 hours.

At 0600 UTC on June 23, a weak cold front entered Alberta near Grande Prairie in the wake of the TROWAL. The front remained relatively stationary until 1800 UTC, when it pushed through central Alberta. By 00:00 UTC on June 24, the front extended from Rocky Mountain House northeast to Lac La Biche. At 0600 UTC, a 1002 mb low formed on this front near Coronation, triggered by the influx of PVA. This low moved rapidly eastward and in 12 hours was entering Manitoba.

The cold front moved southeastward out of Alberta and by 00:00 UTC June 25, a 1022 mb high had formed over central Alberta.

Figures 4.5 through 4.8 show the composite maps covering the period from 00:00 UTC June 23 to 12:00 UTC June 24 when most of the lightning activity occurred. Features of particular interest are the areas of PVA, the position of the TROWAL and associated moisture, the lows that formed in the lee of the Rockies, and the line of convergence that coincided with the low that formed on 0600 UTC June 24.

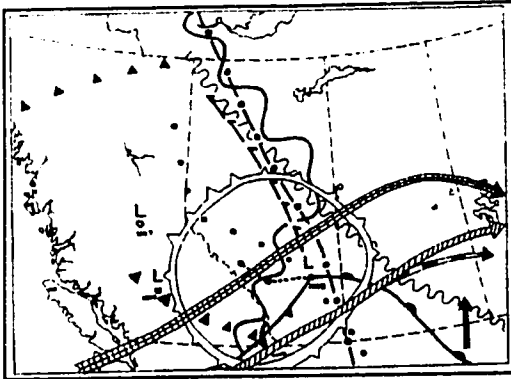


**Figure 4.5.** Composite map for 00:00 UTC June 23, 1988.

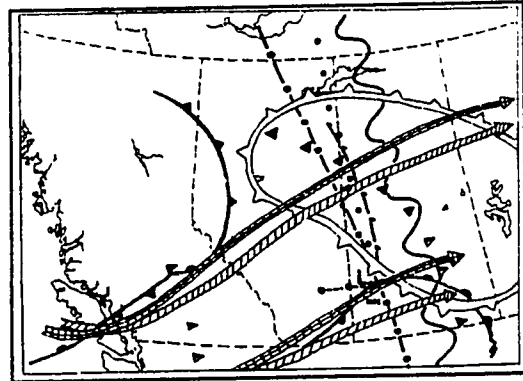


**Figure 4.6.** Composite map for 12:00 UTC June 23, 1988.

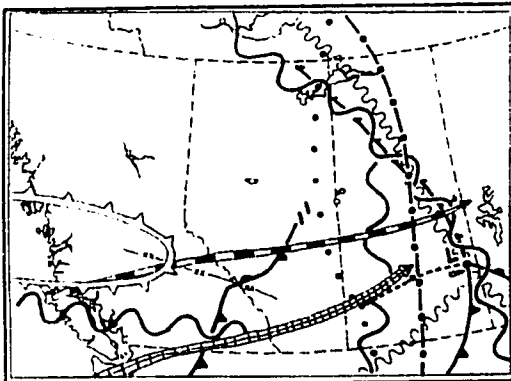


**Figure 4.7.** Composite map for 00:00 UTC June 24, 1988.

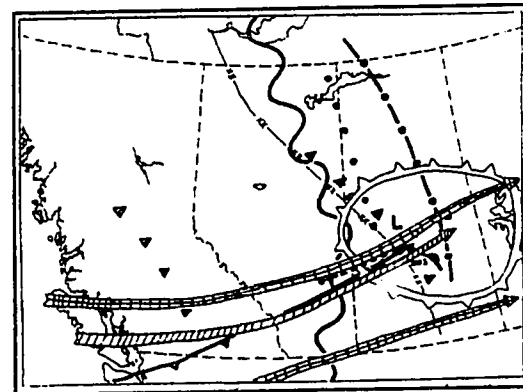


**Figure 4.8.** Composite map for 12:00 UTC June 24, 1988.

Figures 4.9 and 4.10 show the tracks of the major lightning centres for June 22 and 23. Each lightning centre is labelled with a character -- A to G for June 22 and T to Z for June 23. The approximate local time when the centre began is shown inside the circle and the time the centre ended, if before 2400 LDT, is shown at the end of the track.

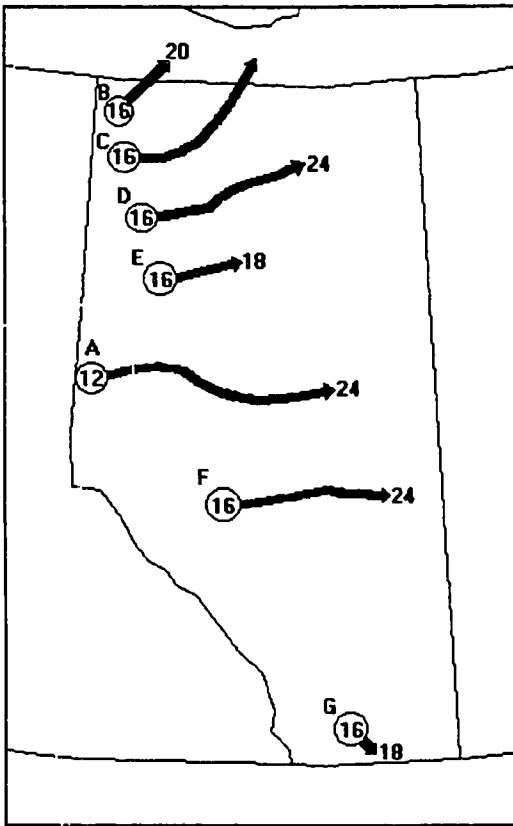


Figure 4.9. Lightning centre tracks for June 22, 1988.

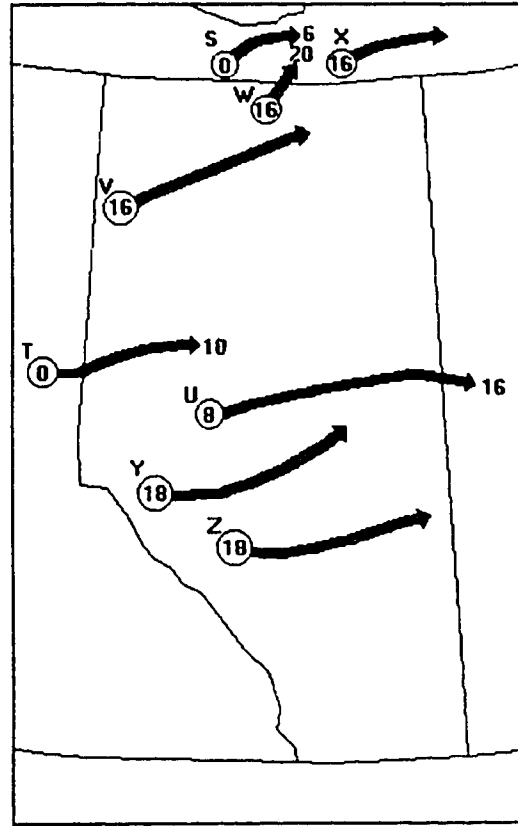


Figure 4.10. Lightning centre tracks for June 23, 1988.

The lightning pattern for June 22 appears to be primarily associated with the TROWAL that moved across Alberta. This is clearly illustrated by centres B through F that formed in a line at 16:00 LDT. Moisture axes at the surface and 850 mb and the 850 mb thermal ridge coinciding with the TROWAL created conditions favorable for convective instability. It is interesting to note that lightning centre G does not appear to have any synoptic explanation and no surface reports suggest that this lightning occurred. A likely explanation is that they are baseline errors -- an error that can occur outside the normal coverage area of detection networks.

Unlike June 22, the lightning on June 23 was caused by several events. Centre S was the continuation of a storm caused by the TROWAL that began the previous afternoon. Centre T formed on the cold front that entered western Alberta. As it died, centre U developed to the southeast and tracked across Alberta into Saskatchewan. At 16:00 LDT, centres V, W, and X formed in the north, likely caused by the TROWAL. The low that formed at 0600 UTC (18:00 LDT) and the influx of PVA that lead to the low's development triggered centres Y and Z.

Figures 4.11 through to 4.16 show the lightning occurrence prediction maps for negative flashes using the logistic regression Model 1 for 12:00 UTC and for 00:00 UTC. These two regression models were used because they had the best skill scores.



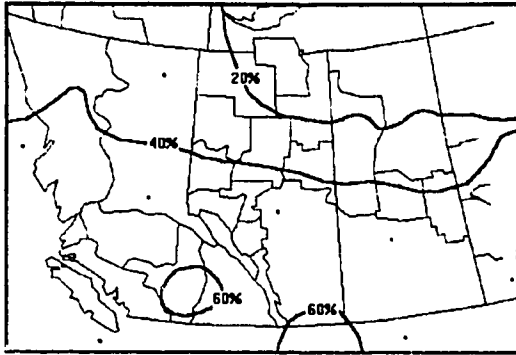


**Figure 4.11.** Negative lightning occurrence prediction map for 12:00 UTC June 22, 1988.

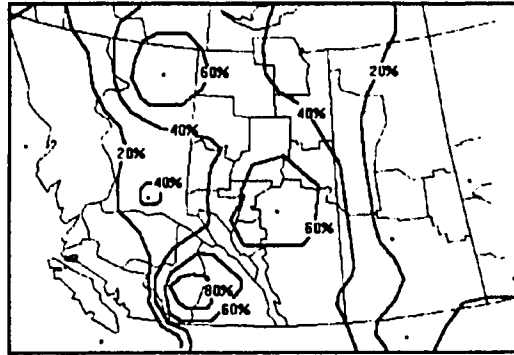


**Figure 4.12.** Negative lightning occurrence prediction map for 00:00 UTC June 23, 1988.

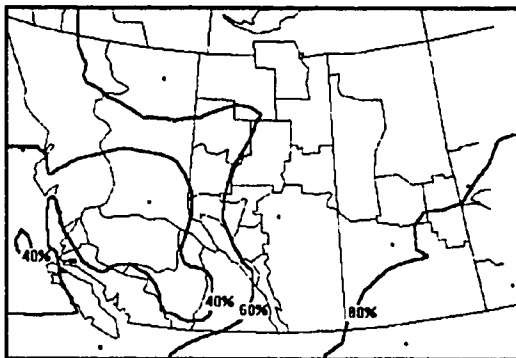


**Figure 4.13.** Negative lightning occurrence prediction map for 12:00 UTC June 23, 1988.

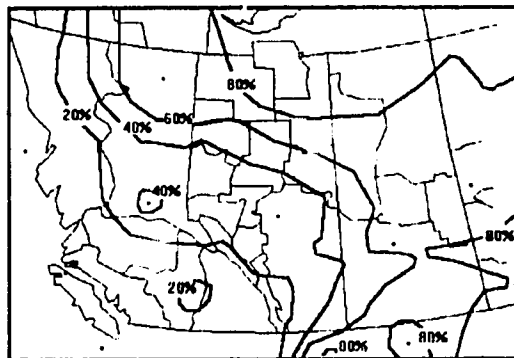


**Figure 4.14.** Negative lightning occurrence prediction map for 00:00 UTC June 24, 1988.

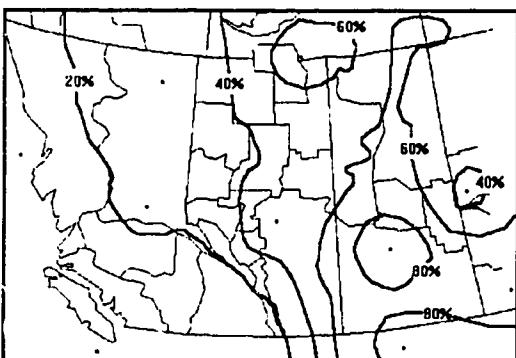


**Figure 4.15.** Negative lightning occurrence prediction map for 12:00 UTC June 24, 1988.

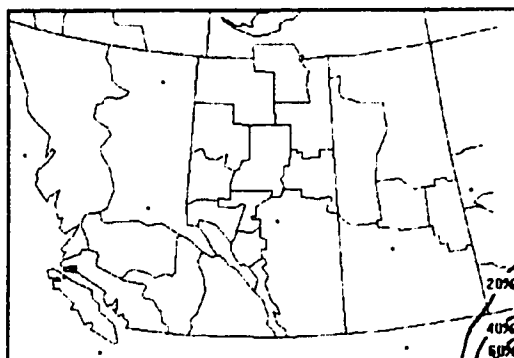


**Figure 4.16.** Negative lightning occurrence prediction map for 00:00 UTC June 25, 1988.

The two regression models emphasize different parameters. For the 12:00 UTC equation, the variables used include the simplified K index and radiation. The 00:00 UTC equation uses the George's K, the 500 mb height changes, the simplified K index, and the surface temperature. Variables are listed in order of importance for both sets of equations. Because some models require the 24-hour changes of some variables, prediction maps for June 21 were not produced.

The maps were produced using the weighted moving averages technique. The number of stations that were used to build each map depended on data availability. The 00:00 UTC maps were built using the data from 20 upper air stations giving good coverage of western Canada. The 12:00 UTC maps were built with the data from only 10 upper stations, primarily from Alberta, B.C., Alaska, and Washington state.

The resulting lightning probability maps reveal some interesting features. The 12:00 UTC map for June 22 shows only moderate probabilities for lightning with peak values in the south of 60%. This may be a lingering effect from the previous day's relative inactivity. The 00:00 UTC map for June 23 predicts centres of lightning activity around Fort Nelson, Edmonton, and Vernon. Except for the centre around Vernon, these correlate with lightning activity remarkably well. The predicted centre around Vernon can be attributed to high George's K values and large height falls following the passage of the ridge. What the model does not see

is that there is no trough following the ridge. Since the 500 mb height falls parameter is attempting to show the passage of a trough, it has, in essence, been fooled by the circumstances.

June 23 saw lightning activity around Fort Smith and with the low that developed near Coronation. The 12:00 UTC map predicts high probabilities (> 60%) for lightning throughout eastern Alberta while the 00:00 UTC map correctly predicts a high probability (> 80%) over Fort Smith, but seriously underestimates the probability of lightning over central Alberta (< 40%). Figure 4.10 shows that by the model's prediction time window of noon to midnight, the lightning centre T had already dissipated and centre U was approaching the Saskatchewan border entering an area of 50% probability. It could be argued that the models handled these centres properly, but centres Y and Z were missed completely. An explanation for this is that the models could not consider the vorticity centre and the associated PVA that crossed Alberta between 00:00 UTC and 12:00 UTC on July 24. Without this parameter, the models did not see the trigger for the synoptic development.

June 24 saw only a small storm over northwestern Saskatchewan. The 12:00 UTC June 24 map still maintains moderate probabilities (40%) over Alberta and higher probabilities over southern Saskatchewan. However, the 00:00 UTC June 25 map correctly predicted little chance of lightning over Alberta.

Over the period covered, the lightning forecast maps were reasonable at predicting the lightning patterns that occurred. They did have some shortcomings that can be accounted for. The models were built from data from a single upper air station (Stony Plain). Because spatial features, such as vorticity advection and upper troughs, cannot be properly interpreted from a sounding, the models fail to see the synoptic picture. It is here that forecasters must use their knowledge of the models and of the situation to put further refinements into the forecast maps. The composite map study provides some of this knowledge.

The composite map study concluded that features that should be used to adjust any spatial prediction models include fronts, low-level convergence, and positive vorticity advection (PVA). Composite maps for 00:00 and 12:00 UTC for June 24 (Figures 4.7 and 4.8) show the passage of all three of these features through central Alberta. This coincides with the development of the low near Coronation and the lightning activity that the predictive models missed. Although the study does not provide firm guidelines telling how much to modify the prediction models, it would appear that if considered, the forecaster could have correctly predicted the lightning in central Alberta on June 23.

A valid criticism is that the overall patterns produced by the models are a bit too broad, especially those produced by the 12:00 UTC equations. This is a result of models that are too simplistic. Lightning is a complex phenomenon that cannot

be explained with just a few predictors. Further refinement of the regression equations and a better link with the composite maps may improve predictions but perhaps what is needed more is a better understanding of the charge generation process in clouds.

## CHAPTER 5

### CONCLUSIONS

#### 5.1 Conclusions

The goal of this research was to build a scheme to forecast lightning over Alberta. This was accomplished through the development of lightning occurrence and lightning frequency prediction models. These models were built using statistical modeling and map analysis.

The first approach was to predict days with lightning. To do this,  $t$  tests and stepwise logistic regressions were conducted. The  $t$  tests showed that convective parameters, such as convective indices, temperatures, and moisture were the variables that best distinguished between days with lightning and days without lightning. The results of the logistic regression models indicate that the potential for predicting lightning occurrence (the detection rate) is above 80%, though high false alarm rates, 30% on average, reduce the value of these predictions.

Linear regression techniques were used to predict lightning flash frequency. Regressions using individual variables showed a large degree of scatter ( $r$ ) but the significance of the correlation coefficient ( $P$ ) indicate that most are not due to chance. Three multiple linear regression models were built using stepwise linear regression to predict lightning frequency using stepwise linear regressions. These

models show that convective indices are the most important parameters to use, but with the best  $r$  squared values between 0.16 to 0.49, they do not sufficiently explain the variation.

To account for spatial features that cannot be drawn from upper air soundings, severe weather composite maps were studied. This study reinforces the importance of convective parameters shown as low-level moisture, surface warming, and instability. Surface fronts, low-level convergence, and positive vorticity advection were recognized as fields that could not be accounted for by upper air soundings.

Finally, a four-day case study was presented. Spatial prediction maps of negative lightning occurrence as derived in the statistical study were produced using a weighted moving averages technique to interpolate upper air predictors. The forecast maps appeared acceptable in that they forecasted most of the areas of lightning activity. If combined with the results from the composite map study, the forecaster can adjust these maps and produce a more reliable lightning occurrence forecast.

These results clearly show that the intensity of convection is the most important process in lightning occurrence and frequency, and that lightning occurrence can be reliably forecasted. A more significant message, though, is that the techniques used in this study were not able to predict lightning frequencies

reliably. Lightning frequency is a variable that has evaded most research on the subject and it comes as no surprise in this thesis that it continues to be evasive.

## **5.2 Further Research**

The work presented in this thesis has shown quite clearly that reliable lightning occurrence forecasts can be produced from the present knowledge. Lightning frequency still stands out as an unresolved issue.

It is possible that lightning frequency is the wrong phenomenon to be investigating. When lightning frequency is examined, each lightning flash is weighted equally with no consideration for the charge exchanged during the flash. If the same analyses were conducted using the total charge exchanged instead of frequency, better results may be obtained. Regrettably, this is not yet measured by current lightning detection systems.

A second avenue for future research would involve refining the models presented. The approach used in this thesis was to produce models to forecast lightning from standard meteorological data available on a regular and reliable basis. The primary source of data used was upper air sounding at mandatory levels. From these data, instability could be judged using the standard convective indices. These indices reinforce the belief that instability is the leading cause of lightning. A possible future direction would be to take a more detailed look at this information,



studying such features as the convective available potential energy (CAPE). A problem with this is that although better correlations will undoubtedly appear, this information would be difficult to interpolate spatially and include in a forecasting model. Perhaps a more practical approach would be to use upper air data at a wider range of levels, such as every 50 or 100 mb. These fields could be more easily interpolated and would provide a better spatial resolution to predict lightning.

Another possible refinement to the models would be to directly incorporate spatial aspects including surface and upper air fields. As seen in the case study, vorticity advection is a field that cannot be ignored. Other fields that trigger convective activity, such as surface wind convergence and moisture flux convergence, could be studied. If fields such as these proved to be good predictors they could be incorporated into the current models, enhancing them greatly.

## BIBLIOGRAPHY

- Andersson, T., A. Andersson, C. Jacobsson, and S. Nilsson, 1989: Thermodynamic indices for forecasting thunderstorms in southern Sweden. *Meteo. Mag.*, **118**, 141-146.
- Chalmer, J.A., 1967: *Atmospheric Electricity*. Pergamon Press, New York, NY, 515 pp.
- Dye, J.F., 1990: Cloud physics and cloud electrification: what are the connections? *16th Conf. on Severe Local Storms/Conf. on Atmospheric Electricity*, Kananaskis Prov. Park, Alta., Amer. Meteo. Soc., 687-691.
- Flannigan, M.D., and M. Wotton, 1989: A study of interpolation methods for forest fire danger rating in Canada. *Can. J. For. Res.*, **19**, 1059-1066.
- Fuquay, D.M., 1980: *Forecasting Lightning Intensity and Associated Weather*. USDA For. Serv. Res. Pap. INT-244, Intermountain For. and Range Exp. Stn., Ogden, UT, 30 pp.
- Golde, R.H., 1977: *Lightning, Volume 1, Physics of Lightning*. Academic Press, London, 496 pp.
- Herrman, B.D., M.A. Uman, R.D. Brantley, and E.P. Krider, 1976: Test of the principle of operation of the wideband magnetic direction finder for lightning return strokes. *J. Appl. Meteo.* **15**, 402-405.
- Holle, R.L., A.I. Watson, J.R. Dougherty, and R.E. Lopez, 1985: Lightning related to echo type in four MCC's on June 3-5, 1985 in the pre-storm area. *14th Conf. on Severe Local Storms*, Indianapolis, IN, Amer. Meteo. Soc., 358-362.
- \_\_\_\_\_, \_\_\_\_\_, R. Ortiz, and R.E. Lopez, 1990: Spatial patterns of lightning, radar echoes, and severe weather in mesoscale convective systems. *16th Conf. on Severe Local Storms/Conf. on Atmospheric Electricity*, Kananaskis Prov. Park, Alta., Amer. Meteo. Soc., 721-726.
- \_\_\_\_\_, \_\_\_\_\_, R.E. Lopez, and D.R. MacGorman, 1988: Cloud-to-ground lightning in the mesoscale convective system on May 20-21, 1979 during SESAME. *15th Conf. on Severe Local Storms*, Baltimore, MD, Amer. Meteo. Soc., 501-504.

- Hunter, S.M., T.J. Schuur, T.G. Marshall, and W.D. Rust, 1990: Electrical and kinematic structure of an Oklahoma mesoscale convective system. *16th Conf. on Severe Local Storms/Conf. on Atmospheric Electricity*, Kananaskis Prov. Park, Alta., Amer. Meteor. Soc., J52-J57.
- Illingworth, A.J., 1983: Review of thunderstorm electrification processes. *Proc. in Atmospheric Electricity*, edited by L.H. Ruhnke and J. Latham, A. Deepak Pub., Hampton, VA, 149-152.
- Iribarne, J.V., and W.L. Godson 1981: *Atmospheric Thermodynamics*. D. Reidel, Boston, MA, 259 pp.
- Janz, B., and N. Nimchuk, 1985: The 500 mb anomaly chart -- a useful fire management tool. *Proc. 8th Conf. on Fire and Forestry Meteorology*. Detroit, MI., Soc. of Amer. For., 233-238.
- Krehbiel, P.R., M. Brook, R.L. Lhermitte, and C.L. Lennon, 1983: Lightning charge structure in thunderstorms. *Proc. in Atmospheric Electricity*, edited by L.H. Ruhnke and J. Latham, A. Deepak Pub., Hampton, VA, 408-410.
- \_\_\_\_\_, R. Tennis, M. Brook, E.W. Holmes, and R. Comes, 1984: A comparative study of the initial sequence of lightning in a small Florida thunderstorm. *7th Intl. Conf. on Atmospheric Electricity*, Albany, NY, Amer. Meteor. Soc., 279-285.
- Krider, E.P., R.C. Nagle, A.E. Pifer, and D.L. Vance, 1980: Lightning direction-finding systems for forest fire detection. *Bull. Amer. Meteor. Soc.*, **61**, 980-986.
- \_\_\_\_\_, \_\_\_\_\_, and M.A. Uman, 1976: A gated, wideband magnetic direction finder for lightning return strokes. *J. Appl. Meteor.*, **15**, 301-306.
- Latham, J., 1981: The electrification of thunderstorms. *Q.J. of the Royal Met. Soc.*, **107(452)**, 277-298.
- Lee, B.S., and K.R. Anderson, 1990: A spatial analysis approach for forest fire preparedness planning. *Proc. 10th Conf. on Fire and Forest Meteorology*, Ottawa, Ont., AES, 339-345.
- Lopez, R.E., R. Ortiz, J.A. Augustine, W.D. Otto, and R.L. Holle, 1990: The progressive development of cloud-to-ground lightning in the early formative stages of a mesoscale convective complex. *16th Conf. on Severe Local Storms/Conf. on Atmospheric Electricity*, Kananaskis Prov. Park, Alta., Amer. Meteor. Soc., 658-662.

- MacGorman, D.R., and W.L. Taylor, 1981: Lightning location relative to storm structure in an Oklahoma thunderstorm. *11th Conf. on Severe Local Storms*, Kansas City, MO, Amer. Meteo. Soc., 314-319.
- \_\_\_\_\_, \_\_\_\_\_, and W.D. Rust, 1984: Some characteristics of lightning in severe storms on the Great Plains of the United States. *7th Intl. Conf. on Atmospheric Electricity*, Albany, NY, Amer. Meteo. Soc., 229-304.
- Mach, D.M., D.R. MacGorman, and W.D. Rust, 1986: Site errors and detection efficiency in a magnetic direction-finder network for locating lightning strikes to ground. *J. Atm. and Oceanic Tech.*, **3**, 67-74.
- Malan, D.J., 1963: *Physics of Lightning*. The English Universities Press Ltd., London, 176 pp.
- Miller, R.C., 1967: *Notes on Analysis and Severe-storm Forecasting Procedures of the Military Weather Warning Centre*. Air Weather Service Technical Report 200, USAF, 158 pp.
- Neter, J., W. Wasserman, and M.H. Kutner, 1985: *Applied Linear Statistical Models*, Irwin, Homewood, IL, 1127 pp.
- Nimchuk, N., 1985: The lightning location and protection (LLP) system: Alberta's operational experience. *Proc. 2nd Central Region Fire Weather Committee Scientific and Technical Seminar*, Winnipeg, Man., Can. For. Serv., Edmonton, Alta., 11-17.
- \_\_\_\_\_, 1983: *Wildfire Behavior Associated with Upper Ridge Breakdown*. ENR Rep No. T/50, Alberta Energy and Natural Resources, Edmonton, Alta., 45 pp.
- Ramsey, G.S., and D.G. Higgins, 1986: *Canadian forest fire statistics/ Statistiques sur les incendies de foret au Canada 1981, 1982, 1983*. Information Report PI-X-49 E/F. Petawawa Natl. For. Inst., Can. For. Ser., Chalk River, Ont., 148 pp.
- Reap, R.M., 1990: Thunderstorms over Alaska as revealed by lightning location data. *16th Conf. on Severe Local Storms/Conf. on Atmospheric Electricity*, Kananaskis Prov. Park, Alta., Amer. Meteo. Soc., J46-J51.
- Reynolds, S.E., M. Brook and M.F. Gourley, 1957: Thunderstorm charge separation. *J. Meteo.*, **14**, 426-436.
- Rust, W.D., and D.R. MacGorman, 1985: Unusual positive cloud-to-ground lightning in Oklahoma storms on 13 May 1983. *14th Conf. on Severe Local Storms*, Indianapolis, IN, Amer. Meteo. Soc., 372-375.

- Simpson, G.C., and G.D. Robinson, 1941: The distribution of electricity in thunderclouds, II. *Proc. R. Soc. (London)*, **A177**, 281-328.
- \_\_\_\_\_, and F.J. Scrase, 1937: The distribution of electricity in thunderclouds. *Proc. R. Soc. (London)*, **A161**, 309-352.
- Sly, W.K., 1966: A convective index as an indicator of cumulonimbus development. *J. Appl. Meteo.*, **5**, 839-846.
- Stolzenburg, M., 1990: Characteristics of the bipolar pattern of lightning locations observed in 1988 thunderstorms. *Bull. Amer. Meteo. Soc.*, **71**, 1331-1338.
- Takeuto, T., S. Isrealsson, M. Nakano, H. Ishkawa, L. Lundquist, and E. Astrom, 1983: On thunderstorms producing positive ground flashes. *Proc. in Atmospheric Electricity*, edited by L.H. Ruhnke and J. Latham, A. Deepak Pub., Hampton, VA, 246-248.
- Uman, M.A., 1987: *The Lightning Discharge*. Academic Press, Orlando, FL, 377 pp.
- \_\_\_\_\_, and E.P. Krider, 1989: Natural and artificially initiated lightning. *Science*, **246**, 457-464.
- \_\_\_\_\_, and \_\_\_\_\_, 1982: A review of natural lightning: experimental data and modeling. *IEEE Transactions on Electromagnetic Compatibility*, **EMC-24(2)**, 79-112.
- Williams, E.R., 1988: Anomalous electrification in winter storms. *15th Conf. on Severe Local Storms*, Baltimore, MD, Amer. Meteo. Soc., 304-308.
- \_\_\_\_\_, 1985: Large-scale charge separation in thunderclouds. *J. of Geoph. Res.*, **90(D4)**, 6013-6025.
- Wilson, C.T.R., 1920: Investigations on lightning discharges and on the electric fields of thunderstorms. *Trans. R. Soc.*, **221A**, 73-115.

## APPENDIX A

### DERIVATION OF THE LIFTED SURFACE TEMPERATURE

An equation for the temperature of a parcel lifted pseudoadiabatically from the surface to 500 mb was derived from data read off a tephigram. These data are summarized in Table A.1.

**Table A.1. Temperatures at selected pressure levels following pseudoadiabatic expansion.**

Temperature (°C)			
1050 mb	1000 mb	950 mb	500 mb
31.4	30.0	28.5	7.2
29.3	28.0	26.3	4.0
27.5	26.0	24.2	1.0
25.6	24.0	22.1	-2.1
23.7	22.0	20.1	-5.4
21.7	20.0	18.1	-8.8
19.9	18.0	16.0	-12.1
17.7	16.0	13.9	-15.5
15.8	14.0	11.8	-19.0
14.0	12.0	9.8	-22.7
12.0	10.0	7.6	-25.7
10.1	8.0	5.7	-28.9
8.2	6.0	3.5	-32.0
6.3	4.0	1.5	-35.1
4.2	2.0	-0.7	-38.0
2.4	0.0	-2.7	-40.9

Temperatures were converted to Kelvin. A nonlinear regression to predict temperature at 500 mb was conducted using the pressure and temperature at each level as predictors and a regression equation of the following format

$$T_{500} = aT\left(\frac{500}{p}\right)^b + c\left(\frac{500}{p}\right)^d \quad (1)$$

where  $T$  and  $P$  are the predictor temperature and pressure and  $a$ ,  $b$ ,  $c$ , and  $d$  are the regression coefficients.

**Table A.2. Nonlinear regression results.**

	$a$ 0.93770
	$b$ 0.713795
	$c$ 10.413369
	$d$ 1.991457
Correlation coefficient $r^2$	0.9995
Estimated mean square error	0.120739

The regression curve explains 99.95 percent of the variance of the 500 mb temperature. The mean error in the predicted temperature is  $\pm 0.346$  degrees. The largest observed residual is 0.72919.

## APPENDIX B

### DERIVATION OF THE LIFTED 850 MB TEMPERATURE

An equation for the temperature of a parcel lifted pseudoadiabatically from 850 mb to 500 mb was derived from data read off a tephigram. These data are summarized in Table B.1.

**Table B.1. Temperatures at selected pressure levels following pseudoadiabatic expansion.**

Temperature (°C)	
850 mb	500 mb
24.8	7.2
22.5	4.0
20.4	1.0
18.2	-2.1
16.1	-5.4
13.8	-8.8
11.5	-12.1
9.4	-15.5
7.1	-19.0
5.0	-22.4
2.7	-25.7
0.2	-28.9
-2.0	-32.0
-4.2	-35.1
-6.4	-38.0
-8.7	-40.9



Temperatures were converted to Kelvin. A polynomial regression to predict temperature at 500 mb was conducted using the 850 mb temperature as the predictor and a regression equation of the following format

$$T_{500} = aT^2 + bT + c \quad (1)$$

where  $T$  is the predictor temperature and  $a$ ,  $b$ , and  $c$  are the regression coefficients.

**Table B.2. Polynomial regression results.**

$a$	0.0042334022
$b$	1.3738456
$c$	-29.12413
Correlation coefficient $r^2$	0.99957
Estimated mean square error	0.14316

The regression curve explains 99.957 percent of the variance of the 500 mb temperature. The mean error in the predicted temperature is  $\pm 0.378$  degrees.

## APPENDIX C

### DERIVATION OF THE ISOBARIC WET-BULB TEMPERATURE

in an adiabatic, isobaric (isenthalpic) process, it can be shown that

$$T + \frac{l_v}{c_p} r = \text{const.} \quad (1)$$

where  $T$  is the dry-bulb temperature and  $r$  is the mixing ratio and assuming  $l_v$  is constant with temperature (Iribarne and Godson 1972).

If we look at the dry-bulb and the wet-bulb temperatures, the equation would become

$$T + \frac{l_v}{c_p} r = T_{iw} + \frac{l_v}{c_p} r_w \quad (2)$$

where  $T_{iw}$  is the isobaric wet-bulb temperature,  $r$  is the saturation mixing ratio at  $T_{iw}$ . Replacing the mixing ratio with

$$r = \frac{\epsilon e(T)}{p} \quad (3)$$

and solving for  $T_{iw}$ , the equation becomes

$$T_{iw} = T + \frac{l_v \varepsilon}{c_p p} [e(T) - e_s(T_{iw})] \quad (4)$$

Replacing the vapor pressure,  $e(T)$ , with the saturation vapor pressure at the dew-point, and using a suitable approximation of the saturation vapor pressure,

$$\log_{10} e_w = 9.4041 - \frac{2354}{T} \quad (5)$$

the finalized form of the equation is

$$T_{iw} = T + 10^{9.4041} \frac{l_v \varepsilon}{c_p p} (10^{-2354/T_d} - 10^{-2354/T_{iw}}) \quad (6)$$

**APPENDIX D**  
**LIGHTNING FREQUENCY FOR STONY PLAIN BETWEEN 12:00 UTC AND 00:00**  
**UTC, 1986**

Day	May		June		July		August	
	Pos	Neg	Pos	Neg	Pos	Neg	Pos	Neg
1	-	-	0	0	0	0	0	0
2	0	0	0	2	5	21	0	3
3	0	0	0	0	24	506	80	1623
4	0	0	0	13	0	5	0	1
5	0	0	0	0	1	7	0	0
6	0	0	5	288	27	152	0	0
7	0	0	36	1582	2	390	15	357
8	4	5	0	0	42	806	0	0
9	0	5	0	0	32	918	0	0
10	0	0	1	46	18	228	0	2
11	5	19	0	0	11	35	19	184
12	0	0	0	0	0	24	10	118
13	7	18	0	0	0	5	0	1
14	0	0	0	8	8	160	4	56
15	0	0	17	75	0	0	0	0
16	0	0	0	0	5	6	0	0
17	0	0	33	208	11	47	0	0
18	0	0	15	356	5	42	0	0
19	0	0	1	4	8	609	0	0
20	0	1	0	0	1	23	0	0
21	4	250	0	0	1	16	0	0
22	0	0	0	0	43	1374	0	0
23	0	0	26	24	1	15	0	0
24	0	0	12	312	50	409	0	1
25	0	0	39	191	2	10	0	0
26	1	14	0	0	42	915	0	0
27	0	0	9	57	3	97	0	0
28	0	1	0	0	42	151	0	0
29	0	0	0	2	0	13	1	1
30	0	0	0	0	9	219	0	0
31	0	0	-	-	0	0	2	8

**APPENDIX E**  
**LIGHTNING FREQUENCY FOR STONY PLAIN BETWEEN 12:00 UTC AND 00:00**  
**UTC, 1987**

Day	May		June		July		August	
	Pos	Neg	Pos	Neg	Pos	Neg	Pos	Neg
1	-	-	0	0	0	0	0	0
2	0	0	0	0	3	2	0	0
3	0	0	0	0	0	1	0	0
4	1	25	0	0	0	0	111	765
5	0	0	88	398	0	0	3	80
6	0	0	3	33	0	0	0	0
7	0	0	0	0	34	666	0	0
8	0	0	0	0	29	234	1	1
9	0	3	32	1428	0	0	0	52
10	0	0	28	63	8	0	0	0
11	0	0	0	0	1	1	0	0
12	3	2	0	0	23	461	0	0
13	0	0	0	0	0	0	0	0
14	0	0	0	0	0	13	0	0
15	0	0	8	4	12	308	0	0
16	0	0	0	0	2	27	4	73
17	0	0	0	0	0	0	1	32
18	7	111	0	0	1	2	12	160
19	0	0	29	752	8	8	1	13
20	0	0	3	116	48	463	14	168
21	0	0	74	162	18	223	0	3
22	0	9	1	14	16	419	0	1
23	2	124	0	0	4	676	3	35
24	1	3	0	0	0	2	18	162
25	0	0	0	0	105	2211	0	0
26	0	0	2	8	0	0	0	0
27	0	1	24	263	1	17	20	202
28	63	790	0	0	0	0	2	0
29	0	0	0	2	26	220	0	0
30	2	0	0	12	217	4379	0	0
31	0	33	-	-	357	3381	0	0

**APPENDIX F**  
**LIGHTNING FREQUENCY FOR STONY PLAIN BETWEEN 12:00 UTC AND 00:00**  
**UTC, 1988**

Day	May		June		July		August	
	Pos	Neg	Pos	Neg	Pos	Neg	Pos	Neg
1	-	-	29	65	0	7	4	32
2	0	0	0	0	36	938	0	0
3	0	0	0	0	1	1	0	1
4	0	0	0	28	0	0	8	107
5	0	0	0	0	0	1	12	6
6	0	0	0	10	1	0	0	0
7	1	0	26	36	2	100	0	0
8	0	0	31	16	0	0	0	0
9	1	0	0	0	14	54	29	171
10	0	0	20	243	2	21	0	0
11	0	0	0	1	0	47	0	11
12	0	0	8	98	12	44	0	0
13	0	9	9	11	43	75	0	5
14	0	0	0	0	14	366	70	51
15	0	0	38	374	13	97	4	31
16	0	0	1	37	0	0	1	0
17	0	0	7	44	0	2	0	0
18	0	0	15	478	9	42	0	13
19	0	0	8	2	0	0	3	88
20	0	0	0	6	0	0	5	19
21	0	0	0	0	0	3	14	23
22	0	0	22	259	2	2	0	0
23	9	5	102	409	0	0	0	0
24	0	1	0	0	0	0	0	0
25	0	1	0	0	0	0	0	1
26	0	0	0	2	0	0	0	0
27	0	2	41	1458	33	139	0	0
28	0	0	12	19	2	29	0	0
29	10	17	2	3	0	14	16	883
30	0	2	0	0	0	0	0	0
31	0	2	-	-	0	0	0	0

**END**

**24·04·92**

**FIN**